1974

Local buckling of cold-formed steel structural members having initially curved compression elements

William M. McKinney

Department:

LOCAL BUCKLING OF COLD-FORMED STEEL STRUCTURAL MEMBERS HAVING INITIALLY CURVED COMPRESSION ELEMENTS

BY

WILLIAM MORRIS MCKINNEY, 1949-

A THESIS

Presented to the Faculty of the Graduate School of the

UNIVERSITY OF MISSOURI-ROLLA

In Partial Fulfillment of the Requirements for the Degree

MASTER OF SCIENCE IN CIVIL ENGINEERING

1974

Approved by

Wei-Wen Yu (Advisor) Wm. A. Andrews

Peter G. Hansen

ABSTRACT

A comprehensive investigation of the effect of initial deviation from flatness on buckling stress and post-buckling strength of compression elements in structural plate members is presented. The study of stiffened and unstiffened elements expands the scope of elastic stability for initially curved plates. Finite element techniques were utilized for the study of unstiffened elements.

ACKNOWLEDGEMENT

Very special thanks are extended to my major advisor, Dr. Wei-Wen Yu, Professor of Civil Engineering, University of Missouri-Rolla not only for his valuable guidance and help, but also for his continued patience and encouragement during the course of this study.

Thanks are also due to Dr. William A. Andrews, Professor of Civil Engineering, and Dr. Peter G. Hansen, Chairman and Professor of Engineering Mechanics, for their advice during preparation of this thesis.

Appreciation is due to Dr. C.S. Davis, Research Engineer of Ford Motor Company, for his advice and suggestions in running the finite element program used.

Appreciation is also extended to American Iron and Steel Institute for the sponsorship of this research project.

TABLE OF CONTENTS

LIST OF ILLUSTRATIONS

LIST OF TABLES

I. INTRODUCTION

A. Origin of Problem

The 1968 Edition of the Specification for the Design of Cold-Formed Steel Structural Members and Addendum No. 1 published by the American Iron and Steel Institute (AISI)(1,2) prescribe the material that can be utilized under this Specification. Both material properties and dimensions of cross sections are limited by the scope of the research on which the Specification is based. Included in Section 1.2 of the Specification are steel sheets and strip with the following ASTM Designations: A245, A374, A375, A446, A570, A606, A607, and A611 (3,4,5, 6,7,8,9,10). This assures that such properties as ductility, weldability, and suitability are consistent with Specification requirements. Also in the AISI Specification, thickness limitations are set at no greater than one-half inch. This upper limit was instituted because the research that has been performed, on which the Specification is based, was carried out on relatively thin steel sheet or strip. These thicknesses usually ranged from 0.03 to 0.10 inch in the Cornell projects with a small amount of work conducted on specimens as thick as one-quarter inch (11). However, in recent years, plates as thick as 2-1/2 inches have been used for some cold-work studies at the Applied Research Laboratories of the United States Steel Corporation (12).

There were several reasons for using the thinner sheets rather than thicker plates in the previous investigations. First, the thinner sheets are actually used more often in cold-formed steel construction

than the thicker sheets and plates. Second, because the larger sections cost more to fabricate and in some cases a proper machine for fabrication was not available, the use of thicker sections was not practical. Third, in view of the fact that the behavior of structural members depends mainly on material properties and dimensional ratios, not necessarily on absolute thickness, the results obtained from the small sections were also assumed representative of the larger sections.

In the past several years, members as thick as 3/4 inch have been successfully cold-formed for structural purposes (13). Such structural applications as truck and car body frames, electrical transmission poles, and heavy construction equipment framing have used the thicker material. With the cold-forming of more and more thicker sections, a specification is needed to cover this larger range of thicknesses. For this reason, a research project was initiated in September 1971 at the University of Missouri-Rolla under the sponsorship of the American Iron and Steel Institute to study the effect of thickness on design requirements.

Probably the most important subjects were in the areas of local buckling and post-buckling strength of plate elements, connection design, the utilization of cold-work, and plastic design. These subjects reflect certain overlapping requirements of the AISI and AISC (American Institute of Steel Construction) Design Specifications (1,14).

One parameter governing local buckling and post buckling strength which might be affected by the thickness of the base metal is the initial deviation from flatness of the compression elements. Initial

deviation from flatness will be considered to take two forms. Shown in Figure 1 is the initial curvature which will reduce the buckling load of the element. The curvature in the longitudinal direction is dominant and reduces the stiffness of the element. Shown in Figure 2 is the initial curvature in the transverse direction. For the critical condition, this type of curvature can be neglected since it increases the buckling load of the element.

B. Purpose of Investigation

The purpose of this investigation is to study the effect of initial deviation from flatness on local buckling and post-buckling strength of stiffened and unstiffened compression elements. Based on analytical investigation and study of existing work, both qualitative and quantitative trends are sought for this relationship. The suitability of using the present AISI requirements for local buckling and post-buckling strength of thick sheets and plates are examined in detail.

The design requirements presently included in the AISI Specification for the buckling and post-buckling strength of flat plates are based on theoretical values supplemented by test results of George Winter at Cornell University (15,16,17) and other investigators (18,19,20). As stated previously, these tests were made on relatively thin material. By determining the interlocking relationships between base metal thickness, initial curvature, and buckling and post-buckling strength, the validity of using the existing test results as a basis for design criteria can be evaluated.

C. Scope of Investigation

This study includes an analytical investigation of the effect of initial deviation from flatness on the buckling and post-buckling strength of compression elements. As an initial step, available publications were reviewed in detail. Chapter II consists of a summary of the literature review. It is divided into a general review of the strength of thin plates in compression and the effect of initial deviation from flatness in particular.

The local buckling and post-buckling of compression elements with initial curvature are discussed in Chapters III and IV.

Finally, Chapter V summarizes the results of this investigation and presents the conclusions derived from this study. The possible impact on design criteria, and recommendations for further study are also included.

The study of the other areas possibly affected by base metal thickness, such as connection design, utilization of cold-work, and plastic design, is beyond the scope of this study.

II. REVIEW OF LITERATURE

A. Introduction

There are a large number of publications which cover the strength of thin plates. Classic solutions for initial buckling of compression elements used "small deflection" theory and are presented in Section B of this chapter.

More extensive work is presented in Section C. The "large-deflection" theory was used to investigate the post-buckling strength. Experimental findings are also presented in this section.

Section D presents a comprehensive review of analytical solutions considering the effect of initial deviation from flatness on the buckling strength of compression elements.

B. Local Buckling of Compression Elements

The classic solution for initial buckling of compression elements has been considered by numerous investigators (21,22). Using "small deflection" theory, either a differential equation approach or an energy approach may be used. In these approaches, deflections are assumed to be small relative to the thickness of the plate. Membrane stresses developed stay within the elastic range.

This type of approach may be utilized for solving different types of compression elements for their initial buckling load. Timoshenko has presented a rigorous solution for several different types of compression elements, including various shapes of plates and boundary conditions (21).

In a thin walled structural member, the isolated compression element has some degree of rotational restraint along its supported

edges. This condition is somewhere between totally fixed and pinned. However, for design purposes the simple supported condition is often used to determine the buckling load, for three reasons: 1) the assumption of simple supports is conservative, 2) the degree of rotational restraint provided by the adjacent element would be difficult to measure, and 3) any rotational restraint may be insignificant for thin sections.

Based on the reasons outlined above, the analytical portion of this study will be limited to rectangular elements with three or four sides simply supported. Uniaxial compression is applied to the transverse edges, both simply supported.

In this study, the definitions of stiffened and unstiffened compression elements are adopted from the AISI Specification (1). The stiffened element is a flat element of which both longitudinal edges are simply supported. The unstiffened element is a flat element which is simply supported along one longitudinal edge with the other longitudinal edge free.

The experimental work reviewed in this study was obtained from structural members, rather than individual plates. For these tests, some rotational restraint was present and influenced the results. This might be taken into account for comparison with analytical results.

The solution of the initial buckling load for both stiffened and unstiffened elements is basic. Because both types of compression elements utilize small deflection theory, they have the same governing equations. Only boundary conditions and the assumed deflected shape

vary. The following discussion deals with the details of the theoretical treatments.

Unstiffened Compression Elements

The buckling stress of unstiffened compression elements can be determined by the differential equation originally derived by Saint Venant in 1883 (23):

$$\frac{\partial^4\omega}{\partial x^4} + 2\frac{\partial^4\omega}{\partial x^2\partial y^2} + \frac{\partial^4\omega}{\partial y^4} = \frac{1}{D}\left[q + \sigma_x t\frac{\partial^2\omega}{\partial x^2} + \sigma_y t\frac{\partial^2\omega}{\partial y^2} + 2\tau_{xy} t\frac{\partial^2\omega}{\partial_x\partial_y}\right] \quad (2.1)$$

where D = the plate flexural rigidity, $Et^3/12(1-\mu^2)$

q = the lateral uniform load applied to the plate

t = the thickness of the plate

ω = the lateral deflection of the plate

σ_x, σ_y = stress components normal to the edges of the plate and lying in the x-y plane

τ_{xy} = the shear stress component on the edges of the plate in the x-z and y-z planes.

The plate configuration for Equation 2.1 is illustrated in Figure 3 with coordinates and stress components.

Eliminating the non-existent stress terms in Equation 2.1, the governing equation is:

$$\frac{\partial^4\omega}{\partial x^4} + 2\frac{\partial^4\omega}{\partial x^2\partial y^2} + \frac{\partial^4\omega}{\partial y^4} = -\frac{\sigma_x t}{D}\cdot\frac{\partial^2\omega}{\partial x^2} \quad (2.2)$$

The sign in front of the σ_x term is changed to indicate that the plate is subjected to a compressive load in the x-direction. Timoshenko (21) assumed that the plate buckled in m half sine waves conforming to the following equation:

$$\omega = f(y) \sin \frac{m\pi x}{a} \tag{2.3}$$

Where a = the length of the plate

$f(y)$ = a function of y alone

Equation 2.3 satisfies the boundary conditions along the simply supported edges x=0 and x=a:

$$\text{at } x = 0,a \quad \begin{cases} \omega = 0 \\ \dfrac{\partial^2 \omega}{\partial x^2} + \mu \dfrac{\partial^2 \omega}{\partial y^2} = 0 \end{cases} \tag{2.4}$$

From Equations 2.2 and 2.3, one can obtain the following expression:

$$\frac{m^4\pi^4}{a^4} f \sin \frac{m\pi x}{a} - 2 \frac{m^2\pi^2}{a^2} \left(\frac{d^2 f}{dy^2}\right) \sin \frac{m\pi x}{a} + \frac{d^4 f}{dy^4} \sin \frac{m\pi x}{a}$$

$$= - \frac{\sigma_x t}{D} f \frac{m^2\pi^2}{a^2} \sin \frac{m\pi x}{a} \tag{2.5}$$

If D_y is substituted for d/dy in Equation 2.5 and the expression is rearranged, the following is the resulting equation:

$$\left[\left(D_y - \frac{m^2\pi^2}{a^2}\right)^2 - \frac{\sigma_x t}{D} \frac{m^2\pi^2}{a^2}\right] f = 0 \tag{2.6}$$

$$\text{Assuming, } \alpha = \sqrt{\frac{m^2\pi^2}{a^2} + \sqrt{\frac{\sigma_x t}{D} \cdot \frac{m^2\pi^2}{a^2}}} \tag{2.7}$$

and $$\beta = \sqrt{-\frac{m^2\pi^2}{a^2} + \sqrt{\frac{\sigma_x t}{D} \cdot \frac{m^2\pi^2}{a^2}}} \qquad (2.8)$$

The substitution of α and β into Equation 2.6 yields the following expression:

$$[(D_y^2 - \alpha^2)(D_y^2 + \beta^2)]f = 0 \qquad (2.9)$$

or $$[(D_y + \alpha)(D_y - \alpha)(D_y^2 + \beta^2)]f = 0 \qquad (2.10)$$

The general solution for the differential Equation 2.10 is:

$$f(y) = C_1 e^{-\alpha y} + C_2 e^{\alpha y} + C_3 \cos \beta y + C_4 \sin \beta y \qquad (2.11)$$

By inspecting the boundary conditions along y=0,w given in Equations 2.12 and 2.13, it can be seen that in Equation 2.11, $C_1 = -C_2$ and $C_3 = 0$.

(a) At y=0

$$\omega = 0 , \quad \frac{\partial^2\omega}{\partial y^2} + \mu \frac{\partial^2\omega}{\partial x^2} = 0 \qquad (2.12)$$

(b) At y=w

$$\frac{\partial^2\omega}{\partial y^2} + \mu \frac{\partial^2\omega}{\partial x^2} = 0, \qquad (2.13)$$

and $$(12)\ \frac{\partial^3\omega}{\partial y^3} + (2-\mu) \frac{\partial^3\omega}{\partial x^2 \partial y} = 0 \qquad (2.14)$$

Assuming $A = 2C_1$ and $B = C_1$ and changing the e functions to hyperbolic functions, Equation 2.11 becomes:

$$f(y) = A \sinh \alpha y + B \sin \beta y \tag{2.15}$$

By substituting expressions 2.3 and 2.15 for ω and $f(y)$ into Equations 2.13 and 2.14, the following two simultaneous equations can be found:

$$A(\alpha^2 - \mu \frac{m^2\pi^2}{a^2}) \sinh \alpha w - B(\beta^2 + \mu \frac{m^2\pi^2}{a^2}) \sin \beta w = 0 \tag{2.16}$$

$$A\alpha[\alpha^2-(2-\mu) \frac{m^2\pi^2}{a^2}] \cosh \alpha w - B\beta[\beta^2+(2-\mu) \frac{m^2\pi^2}{a^2}] \cos \beta w = 0 \tag{2.17}$$

These two simultaneous equations are satisfied if A=B=0, which would result in no lateral deflection. The equations are also satisfied if the determinate of the coefficients of the unknowns A and B is zero, i.e.

$$(\alpha^2 - \mu \frac{m^2\pi^2}{a^2}) \sinh \alpha w\beta[\beta^2+(2-\mu) \frac{m^2\pi^2}{a^2}] \cos \beta w$$

$$-(\beta^2 + \mu \frac{m^2\pi^2}{a^2}) \sin \beta w\alpha[\alpha^2-(2-\mu) \frac{m^2\pi^2}{a^2}] \cosh \alpha w = 0 \tag{2.18}$$

By rearranging some of the terms, Equation 2.18 can be simplified as follows:

$$(\alpha^2 - \mu \frac{m^2\pi^2}{a^2}) \tanh \alpha w - (\beta + \mu \frac{m^2\pi^2}{a^2})^2 \tan \beta w = 0 \tag{2.19}$$

By defining plate dimensions and material properties, Equations 2.7, 2.8, and 2.19 can be used to determine the critical buckling stress, σ_{cr}. These equations have been solved for σ_{cr}. The following general

equation is used with a buckling coefficient, K.

$$\sigma_{cr} = \frac{K\pi^2 D}{tw^2} \tag{2.20}$$

Because of the difficulty in solving Equation 2.19, Bulson (22) has used a computer solution. His results are shown as a solid curve in Figure 4. Unlike the stiffened plate, the unstiffened plate does not take the "Garland" form as described in reference 22. The plate should buckle in a single half sine wave regardless of the length to width ratio. Both Timoshenko and Bulson have presented an energy solution which is close to the exact solution. The coefficient K was found to be

$$K = \frac{w^2}{a^2} + \frac{6(1-\mu)}{\mu^2} \tag{2.21}$$

This solution is shown as a dashed curve in Figure 4 for the purpose of comparison.

Stiffened Compression Elements

The same governing Equation 2.2 can be used for stiffened plates, the only difference being the assumed deflected shape. The equation conforming to the buckled shape of a stiffened plate is:

$$\omega = f(y) \sin \frac{m\pi x}{a} \tag{2.22}$$

where $f(y) = A_1 \cosh \alpha y + A_2 \sinh \alpha y + A_3 \cos \beta y + A_4 \sin \beta y$. Bulson (22) has solved these differential equations and obtained the following solution:

$$-(r_1^2 + s^2) \sinh p \sin q_1 = 0 \tag{2.23}$$

where

$$p = \left[\frac{m\pi^2}{\phi}(\sqrt{k} + \frac{m}{\phi})\right]^{1/2} \tag{2.24}$$

$$q_1 = \left[\frac{m\pi^2}{\phi}(\sqrt{k} - \frac{m}{\phi})\right]^{1/2} \tag{2.25}$$

and,
$$r_1^2 = p^2 - \mu \frac{m^2\pi^2}{\phi^2} \tag{2.26}$$

$$s^2 = q_1^2 + \mu \frac{m^2\pi^2}{\phi^2} \tag{2.27}$$

$$\phi = \frac{a}{w}$$

The solution can be expressed in the following form of a relationship between K and ϕ:

$$K = \frac{1}{\phi^2} + \phi^2 + 2 \tag{2.28}$$

Figure 5 shows this relationship plotted for several ϕ ratios. This type of relationship is known as the Garland form. As can be seen, the minimum K factor is 4.0 and occurs when ϕ is an integer. For long plates $\phi \cong m$, consequently the mode is changed each time when the ϕ ratio is increased by one. This implies that long plates hinged along their longitudinal edges buckle approximately into squares.

C. Post-Buckling Strength of Compression Elements

When compression elements are designed against local buckling, it is desirable to use as much of their strength as possible for better economy. Because stiffened plates show a large amount of strength in the post-buckling range, they are usually allowed to pass

the initial buckling state for prediction of the ultimate strength. It means that they may have a lateral deflected shape as shown in Figure 6. This added strength is due to the membrane stresses developed in the transverse direction. They act as hoop stresses restraining the lateral displacement caused by the longitudinal load.

Unlike stiffened compression elements, the design of unstiffened compression elements is presently based on the initial buckling load except for elements having large width-thickness ratios. There are indications that in the future, the design of unstiffened compression elements will also be based on their post buckling strength (40).

To analyze the plate in this post-buckling range and to take into account these membrane stresses, von Karman developed "large deflection" equations in 1910 (24). Even though a stiffened element may have some rotational restraint, a simply supported condition was used for simplicity. The simplification gives a conservative result. The basic assumptions used in the analysis were: a) deflections are large relative to the plate thickness, b) membrane strains are present during bending, c) plane sections rotating during bending remain normal to the neutral surface and do not distort, d) resistance by the bending moments is dominant and shearing forces are neglected, and e) the plate thickness is small relative to other dimensions.

In this analysis, the x, y, and z axes and u, v, ω displacements correspond to the longitudinal, transverse, and normal directions originating from a point on the middle surface of the plate. This is illustrated in Figure 7. The resultant lateral deflection in

the z direction, ω, is assumed as a double half sine wave function:

$$\omega = \sum_{m=1}^{\infty} \sum_{n=1}^{\infty} a_{mn} \sin \frac{m\pi x}{a} \sin \frac{n\pi y}{w} \tag{2.29}$$

where ω = the resultant deflection in the z direction at coordinates (x,y)

a_{mn} = the amplitude of the sine wave

m = the number of half sine waves in the x direction

n = the number of half sine waves in the y direction

a = the length of the plate

w = the width of the plate

The summation signs denote the different buckling wave patterns the plate could take. Theoretically an infinite number of patterns are possible as shown in Figure 8. But only the first several patterns are critical and need to be considered as will be shown later.

The strains in the middle surface of the plate can be expressed as:

$$\varepsilon_x = \frac{\partial u}{\partial x} + \frac{1}{2} \left(\frac{\partial \omega}{\partial x}\right)^2 \tag{2.30}$$

$$\varepsilon_y = \frac{\partial v}{\partial y} + \frac{1}{2} \left(\frac{\partial \omega}{\partial y}\right)^2 \tag{2.31}$$

and, $$\gamma_{xy} = \frac{\partial u}{\partial y} + \frac{\partial v}{\partial x} + \frac{\partial \omega}{\partial x} \cdot \frac{\partial \omega}{\partial y} \tag{2.32}$$

Differentiating and combining the above strain expressions and substituting in the stress-strain relations satisfying Hooke's Law for two dimensions yields:

$$\frac{\partial^2 \sigma_x}{\partial y^2} - \mu \frac{\partial^2 \sigma_y}{\partial y^2} + \frac{\partial^2 \sigma_y}{\partial x^2} - \mu \frac{\partial^2 \sigma_y}{\partial x^2} - 2\mu \frac{\partial^2 \tau_{xy}}{\partial x \partial y}$$

$$= E\left[\left(\frac{\partial^2 \omega}{\partial x \partial y}\right)^2 - \left(\frac{\partial^2 \omega}{\partial x^2}\right)\left(\frac{\partial^2 \omega}{\partial y^2}\right)\right] \qquad (2.33)$$

where E = modulus of elasticity

μ = Poisson's ratio

Using the differential equation describing the deflection surface originally derived by Saint Venant in 1883 (23),

$$\frac{\partial^4 \omega}{\partial x^4} + 2 \frac{\partial^4 \omega}{\partial x^2 \partial y^2} + \frac{\partial^4 \omega}{\partial y^4} = \frac{1}{D}\left[q + \sigma_x t \frac{\partial^2 \omega}{\partial x^2} + \sigma_y t \frac{\partial^2 \omega}{\partial y^2}\right.$$

$$\left. + 2 \tau_{xy} t \frac{\partial^2 \omega}{\partial x \partial y}\right] \qquad (2.34)$$

The above equation is the same as Equation 2.1.

Introducing the Airy's stress functions:

$$\sigma_x = \frac{\partial^2 F}{\partial y^2} \qquad (2.35)$$

$$\sigma_y = \frac{\partial^2 F}{\partial x^2} \qquad (2.36)$$

$$\tau_{xy} = - \frac{\partial^2 F}{\partial x \partial y} \qquad (2.37)$$

into Equations 2.33 and 2.34 yields:

$$\frac{\partial^4 F}{\partial x^4} + 2 \frac{\partial^4 F}{\partial x^2 \partial y^2} + \frac{\partial^4 F}{\partial y^4} = E\left[\left(\frac{\partial^2 \omega}{\partial x \partial y}\right)^2 - \frac{\partial^2 \omega}{\partial x^2} \cdot \frac{\partial^2 \omega}{\partial y^2}\right] \qquad (2.38)$$

$$\frac{\partial^4\omega}{\partial x^4} + 2\frac{\partial^4\omega}{\partial x^2\partial y^2} + \frac{\partial^4\omega}{\partial y^4} = \frac{t}{D}\left[\frac{q}{t} + \frac{\partial^2 F}{\partial y^2}\cdot\frac{\partial^2\omega}{\partial x^2} + \frac{\partial^2 F}{\partial x^2}\cdot\frac{\partial^2\omega}{\partial y^2}\right.$$

$$\left. -2\frac{\partial^2 F}{\partial x\partial y}\cdot\frac{\partial^2\omega}{\partial x\partial y}\right] \qquad (2.39)$$

Together with the boundary conditions, Equations 2.38 and 2.39 form the basic simultaneous equations governing the elastic behavior of the plate.

Since the basic equations are fourth order and non-linear, the solution is difficult. For this reason early studies used an approximate method, usually an energy solution. Researchers carrying out such studies were Schnadel (25), Cox (26), Timoshenko (21), and Marguerre (27). A deflection surface was assumed and the strain energy due to bending and membrane action was evaluated.

Samuel Levy (28) was the first to present a rigorous solution of von Karman's "large deflection" equations in 1942. He considered the case of simply supported rectangular flat plates under combined edge compression and lateral loading. His results compared favorably with previous researchers. Levy also studied the convergence of the solution as the number of the assumed deflection configurations increased. It was found that the use of the first three deflection configurations in the double harmonic deflection series was sufficient in arriving at an accurate solution.

In 1932, an important paper by von Karman, Sechler, and Donnell was published (29). An approximate analytical method was used to arrive at the ultimate strength of a thin plate. In this study, the

authors used the concept of "effective width" to describe the buckling model. The "effective width" concept refers to a method whereby instead of using the full section of the compression element with a varying stress distribution, a reduced section is used with a constant stress. It was found that

$$P_{ult} = Ct^2\sqrt{E\,\sigma_y} \tag{2.40}$$

where $C = \dfrac{\pi}{\sqrt{3(1-\mu^2)}}$

In this method, the effective width combined with a constant stress was to replace the "non-uniform" stress distribution after exceeding the initial buckling load. The effective width may be considered as a particular width of the plate which just buckles when the compressive stress reaches the yield point of the material, i.e.

$$\sigma_{cr} = \sigma_y = \frac{K\pi^2 E}{12(1-\mu^2)\left(\frac{w}{t}\right)^2} \tag{2.41}$$

where σ_{cr} = critical buckling stress

E = modulus of elasticity

μ = Poisson's ratio

t = thickness of the plate

w = flat width of the plate

K = buckling coefficient

By using $K = 4.0$, $\mu = 0.3$, and $b = w$ for a stiffened plate, Equation 2.42 can be obtained.

$$b/t = 1.90\sqrt{\frac{E}{\sigma_y}} \qquad (2.42)$$

George Winter has performed extensive tests for the compression strength of thin plates at Cornell University. Since 1947, Winter has reported on the local buckling characteristics of both stiffened and unstiffened compression elements (15,16,17). His test data was compared with previous researcher's work. It was found that for cold-formed steel members, the constant of 1.90 used in Equation 2.42 should be modified as follows:

$$1.90\left(1 - \frac{0.475}{w/t}\sqrt{E/f_{max}}\right)$$

Consequently, the resulting equation for computing the effective width of stiffened elements was

$$\frac{b}{t} = 1.9\sqrt{\frac{E}{f_{max}}}\left(1 - \frac{0.475}{w/t}\sqrt{\frac{E}{f_{max}}}\right) \qquad (2.43)$$

As can be seen, Winter's formula for the effective width is similar to von Karman's equation, with the addition of the experimental modification factor

$$1 - \frac{0.475}{w/t}\sqrt{\frac{E}{f_{max}}}$$

After twenty years of successful use of Equation 2.43, it was found that Winter's formula was slightly conservative. Based on the experience gained in the design of cold-formed steel members, Equation 2.43 was modified in 1968. The basic equation for the AISI Specification now reads:

$$\frac{b}{t} = 1.9\sqrt{\frac{E}{f_{max}}}\left[1 - \frac{0.415}{w/t}\sqrt{\frac{E}{f_{max}}}\right] \tag{2.44}$$

As discussed in Winter's Commentary on the Specification (11), the modification brought as much as 10% increase in effective width.

D. Initially Curved Compression Elements

In 1938, Marguerre presented a paper (30) which extended von Karman's "large deflection" equations to include the effect of initial deviation from flatness. Marguerre instituted the type of curvature as shown in Figure 1, where the longitudinal curvature is dominant. The initial deflection surface was considered to be a double half sine wave as given in Equation 2.45:

$$\omega_o = \sum_{m=1}^{\infty}\sum_{n=1}^{\infty} \omega_{o_{mn}} \sin\frac{m\pi x}{a} \sin\frac{n\pi y}{w} \tag{2.45}$$

where ω_o = the initial deflection in the z direction at coordinates (x,y)

$\omega_{o_{mn}}$ = the amplitude of the sine wave; m, n, a and w were previously defined

Consequently, Equations 2.38 and 2.39 become:

$$\frac{\partial^4 F}{\partial x^4} + 2\frac{\partial^4 F}{\partial x^2 \partial y^2} + \frac{\partial^4 F}{\partial y^4} = E\left[\left(\frac{\partial^2 \omega}{\partial x \partial y}\right)^2 - \frac{\partial^2 \omega}{\partial x^2}\cdot\frac{\partial^2 \omega}{\partial y^2}\right.$$

$$\left. - \left(\frac{\partial^2 \omega_o}{\partial x \partial y}\right)^2 + \frac{\partial^2 \omega_o}{\partial x^2}\cdot\frac{\partial^2 \omega_o}{\partial y^2}\right] \tag{2.46}$$

$$\frac{\partial^4(\omega-\omega_o)}{\partial x^4} + 2\frac{\partial^4(\omega-\omega_o)}{\partial x^2\partial y^2} + \frac{\partial^4(\omega-\omega_o)}{\partial y^4} = \frac{t}{D}\left[\frac{q}{t} + \right.$$

$$\left.\frac{\partial^2 F}{\partial y^2}\cdot\frac{\partial^2\omega}{\partial x^2} + \frac{\partial^2 F}{\partial x^2}\cdot\frac{\partial^2\omega}{\partial y^2} - 2\frac{\partial^2 F}{\partial x\partial y}\cdot\frac{\partial^2\omega}{\partial x\partial y}\right] \qquad (2.47)$$

This development finally made it possible to study the effect of initial deviations on plate bending with an exact method.

In 1946, Hu, Lundquist, and Batdorf published a paper (31) using Levy's solution of von Karman's "large deflection" equations to study the effect of initial curvature on buckling of plates. In this study, Marguerre's modification of von Karman's equations was used. This was the first paper concerning the effect of initial curvature on buckling and post-buckling of plates known to the author. The simply supported square plate under uniaxial compression was studied for different degrees of intial curvature.

As shown in Figure 1, the degrees of initial deviation from flatness are defined by the amplitude of the sine wave as a fraction of the thickness (t) of the plate. Initial deviations of 0.04 t and 0.1 t were studied by Hu, et al. The most important finding was the effect of the initial deviation on the effective width of the plate. The effective width was defined by the authors as:

$$b = \frac{\bar{\sigma}_a/\sigma_{crx}}{\bar{\varepsilon}_a/\varepsilon_{crx}}\, w \qquad (2.48)$$

where b = the effective width

w = the actual width

$\bar{\sigma}_a$ = the average edge compression in the x-direction

σ_{crx} = the critical stress of the flat plate

$\bar{\epsilon}_a$ = the unit plate shortening in the x-direction

ϵ_{crx} = the critical strain in the x-direction for a flat plate subjected to compression stress in the x-direction

It was found that the intial curvature lowered the buckling and post-buckling stress of the plate. The maximum decrease in strength was found around the initial buckling stress.

J.M. Coan in 1951 also extended Levy's solution of von Karman's "large deflection" equations to include initial deviation (32). An initial deviation of 0.1 t was studied on a simply supported rectangular plate. As in the work of Hu, et al., several load-deflection curves were presented as a result of the study (31).

N. Yamaki published a paper in 1959 (33), which extended the work of Levy and Coan by including more boundary conditions. Load-deflection curves are presented for both flat plates and an initial deviation of 0.1 t. Yamaki also increased the number of deflection configurations from three in Coan's solution to four, which is considered to be more accurate.

More recently, in 1969 Abdel-Sayed presented an approximate theoretical approach for the simply supported square plate (34). The longitudinal edges are restrained to remain straight or are free to move in the plane of the plate. A flat plate was considered

first, followed by an initially curved plate. The effect of initial curvature on the effective width was also examined. Results obtained by Abdel-Sayed qualitatively agree with those of Hu, et al and Coan, previously mentioned. The solution basically only considered the first deflection configuration in von Karman's "large deflection" equations.

In 1971, T.Y. Yang published a paper (35) presenting an approximate solution for the stiffened element. He developed a computer program to solve stability problems by utilizing the finite element method. In his paper, he also presented load-deflection curves for various initial deviations (δ_o/t = 0.0, 0.05, 0.1, and 0.5). The results were compared favorably with the values of Hu, et al. As far as the stiffened plate is concerned, Yang's results only gave an indication of the effect of initial curvature on post-buckling strength because it can only be used up to the initial buckling stress.

In 1972, Dawson and Walker used the same type of approach as done by Abdel-Sayed to consider the effect of initial curvature (36). The first three deflection configurations in von Karman's equations were used instead of the one used in Abdel-Sayed's paper. This paper presents examples that were solved by Coan, Yamaki, and Abdel-Sayed. Good agreements have been obtained between experimental results and the analytical results for initial deviations of 0.0 t and 0.1 t.

The review of literature presented above deals mainly with the type of compression element for which longitudinal curvature is dominant. Because this type of imperfection causes a reduction in

buckling stress and post-buckling strength, it is of great importance for structural design. On the other hand, transverse curvature, as shown in Figure 2 tends to increase the buckling stress and post-buckling strength (37,41), and is therefore relatively unimportant for the instability problems in this investigation.

In 1965, Bruhn published a book containing a study of the effect of transverse curvature on the stiffness of a stiffened plate (37). He used the small deflection linear theory to find the buckling stress of the curved panels from a range of zero curvature to r/t = 3,000. His analytical results are shown in Figure 9, in which the buckling coefficient k was plotted versus the non-dimensional parameter z as defined below.

$$z = \frac{L^2}{rt}(1-\mu^2)^{1/2}$$

In the above, r = the radius of curvature in the transverse direction

L = length of the curved panel

It can be seen that the critical buckling stress increases as the curvature of the panel increases.

It has been indicated by Bruhn that his analytical results have compared favorably with the experimental results. For design purposes, the reduced values of k have been recommended for large ratios of r/t as shown in Figure 9.

As discussed above, a considerable amount of work has been done on the stability of initially curved stiffened compression elements. However, little or no analytical study has been published, to the

author's knowledge, for the effect of initial curvature on the stability of unstiffened elements. It appears that the lack of information on the unstiffened elements was mainly due to the difficulty in solving the extremely complex equations that govern the buckling behavior. For this reason, an approximate method seems to be desirable.

During the past, some researchers have made general statements regarding the effect of initial curvature on unstiffened plates. For example, Cox has indicated in his report (26) that a reduction of the buckling stress should be expected. This stress reduction would be most pronounced around the theoretical buckling stress of the plate. It is the same effect that initial curvature has on stiffened plates. This stress reduction is considered to be more important for unstiffened elements because the load-carrying capacity of the unstiffened elements is usually dependent on the buckling stress of the element, while stiffened plates are often based on the post-buckling strength.

III. STIFFENED COMPRESSION ELEMENTS

A. Statement of Problem

As discussed in Chapter II, the stiffened compression elements will not necessarily fail when the buckling stress is reached. An additional load can be carried by the element after buckling by means of redistribution of stress. Based on the post-buckling strength of the plate, the effective design width method has been used in the AISI design Specification since 1946. Beginning in 1969, the AISC Specification also included design provisions on effective width design for slender compression elements.

During the past, several researchers have investigated the effect of the initial curvature on the effective width of stiffened elements for the ratios of δ_o/t from 0.04 t to 0.3 t (31-35). In this study, it was intended to compare various methods used for determining the effective width and to further investigate the influence of the initial deviation from flatness on the effective design width for δ_o/t ratios up to 1.0 t by using Abdel-Sayed's method.

B. Method of Solution

For computation of the effective design width, two solutions have been developed by Abdel-Sayed depending on the assumed dominant stress (34). Figure 10 shows the plate geometry with respect to the local coordinates used by Abdel-Sayed. Unlike the coordinates used in Figure 3, in Figure 10 the origin was chosen to be located at the centroid of the plate and the compression stress is applied in the y direction. It was assumed that the deflection surface conforms to a cosine function; i.e.

$$\omega = e \cos \frac{\pi x}{w} \cos \frac{\pi y}{a} \tag{3.1}$$

where e is the amplitude of the cosine wave.

The boundary conditions are as follows:

1) Because there is no moment along four edges, at $x = \pm w/2$, $\omega = M_x = 0$, and at $y = \pm a/2$, $\omega = M_y = 0$

2) Because each plate has approximately the same distribution of stresses, at $y = \pm a/2$, v = constant

3) Because the longitudinal edges are allowed to move freely in the plane, at $x = \pm w/2$, $N_x = 0$.

In Reference 34, Abdel-Sayed found that the stress function (F) expressed in Equation 3.2 satisfies the above three boundary conditions, i.e.

$$F = \frac{N_a}{2} x^2 - \frac{Et}{32} (e^2 + 2ee_0)\left[(\frac{w}{a})^2 \cos \frac{2\pi}{w} x + (\frac{a}{w})^2 \cos \frac{2\pi y}{a} \right]$$

$$+ \frac{Et}{32} (e^2 + 2ee_0)(M \cosh \frac{2\pi x}{a} + N \frac{2\pi x}{a} \sinh \frac{2\pi x}{a}) \cos \frac{2\pi y}{a} \tag{3.2}$$

where

$$N = -(\frac{a}{w})^2 \frac{\sinh \frac{\pi w}{a}}{\frac{\pi w}{a} + \cosh \frac{\pi w}{a} \sinh \frac{\pi w}{a}}$$

$$M = (\frac{a}{w})^2 \frac{\frac{\pi w}{a} \cosh \frac{\pi w}{a} + \sinh \frac{\pi w}{a}}{\frac{\pi w}{a} + \cosh \frac{\pi w}{a} \sinh \frac{\pi w}{a}}$$

N_a = average loading per unit width of plate

e = the net deflection in the z direction

e_o = the initial deflection in the z direction

By substituting the above stress function in Equations 2.38 and 2.39, the maximum loading per unit length at $x = \pm w/2$ and $y = 0$ was found to be

$$(n_y)_{max} = N_a + 2(N_a - N_{cr} \frac{e}{e+e_o}) \frac{\pi}{\pi-1} \tag{3.3}$$

where $(n_y)_{max}$ = the maximum loading per unit length in the y direction

N_{cr} = the critical buckling load per unit width determined by $\frac{\pi^2 E t^3}{12(1-\mu^2)w^2}$

The average loading per unit length acting in the y direction was found to be

$$(\bar{n}_y) = N_a + (N_a - N_{cr} \frac{e}{e+e_o}) \frac{\pi}{\pi-1} \tag{3.4}$$

Depending on the stress assumed to be dominant, the effective width to actual width ratio can be found. One of the solutions was arrived at by assuming

$$b/w = N_a/\bar{n}_y$$

$$\frac{b}{w} = \frac{1}{7.469} [\, 1 + 1.465 \frac{N_{cr}}{\bar{n}_y} (\frac{e}{e+e_o}) \,] \tag{3.5}$$

If the deformation along the $x = w/2$ is considered to be governing, then $b/w = N_a/(n_y)_{max}$. Then

$$\frac{b}{w} = \frac{1}{3.93} [\, 1 + 2.93 \frac{N_{cr}}{(n_y)_{max}} (\frac{e}{e+e_o}) \,] \tag{3.6}$$

The procedure used to solve the b/w ratio was discussed by Abdel-Sayed in Reference 34. First, the material properties (E,μ) and the degree of initial deviation from flatness ($k_o = \delta_o/t$) for the case study are defined. The net deflection can then be calculated for a given load level (k) by using Equation 3.7, 3.8, and 3.9.

$$z_1 = (S_1 + S_2) - \frac{a_2}{3} \tag{3.7}$$

$$z_2 = -\frac{1}{2}(S_1 + S_2) - \frac{a_2}{3} + \frac{i\sqrt{3}}{2}(S_1 - S_2) \tag{3.8}$$

$$z_3 = -\frac{1}{2}(S_1 + S_2) - \frac{a_2}{3} - \frac{i\sqrt{3}}{2}(S_1 - S_2) \tag{3.9}$$

where $z = e/t$

$a_2 = 3\theta$

$S_1 = [r + (q^3 + r^2)^{1/2}]^{1/3}$

$S_2 = [r - (q^3 + r^2)^{1/2}]^{1/3}$

In the above expressions,

$q = a_1/3 - a_2^2/9$

$r = (a_1 a_0 - 3a_0)/6 - a_2^3/27$

$a_0 = \phi' k\theta$

$a_1 = 2\theta^2 + (k-1)\phi'$

and $\theta = e_o/t$

$k = N_a/N_{cr}$

$$\phi = -3.92/(1-\mu^2)$$

The largest positive real value of the deflection should be chosen as the most critical condition. Once the net deflection, z, is found for a given load level, the values of $(n_y)_{max}$ and $\bar{n}_y$ can be found from Equations 3.3 and 3.4, respectively. Depending on the assumed dominant stress, Equation 3.5 or 3.6 can be used to calculate the b/w ratio. By increasing the load level, k, a full range of values of the effective width can be calculated.

C. Presentation of Results

This study considered a square plate with four simply supported edges. A modulus of elasticity of 29,500 ksi and Poisson's ratio of 0.3 were used in the numerical calculation. The degrees of initial deviation from flatness of 0.04 t, 0.1 t, 0.2 t, 0.3 t, 0.5 t, 0.7 t, and 1.0 t were investigated. Both Equations 3.5 and 3.6 were used to find the b/w ratio. Figure 11 shows the maximum lateral deflection plotted versus average edge compression based on Equation 3.5. As expected, the initial curvature reduced the buckling stress with its greatest effect at the initial buckling load. A comparison of these results and other researchers' work shows remarkable resemblance. Figure 12 is reproduced from a paper published by Yang (35). In this figure, Yang's finite element results are presented as dashed curves, the results of Hu, et al are indicated as solid lines. It can be seen that the results shown in Figure 11 are remarkably agreeable with those in Figure 12. Note that for $k_o = 0.04$, when the edge compressive load reaches 90% of the bifurcation load for a flat plate, Figure 11

gives approximately 0.3 in/in for $(\delta-\delta_o)/t$ while Figure 12 gives approximately 2.5 in/in. This comparison would indicate the validity of Abdel-Sayed's solution for the net center deflection. Particular notice should be made to the decreasing effect of initial imperfection as the ratio of δ_o/t increases. At $k_o = 1.0$, the load-deflective relationship is almost linear in the initial buckling range.

Using Equations 3.5 and 3.6, the effective widths of initially curved stiffened elements were calculated for the general range of w/t from 33 to 202. The results are tabulated in Table I. As expected, the effective width decreases as the initial deviation increases for certain given values of w/t ratios.

The results obtained from Equations 3.5 and 3.6 are plotted in Figure 13 and 14, respectively. Although they show the same general trends, the results obtained from Equations 3.5 and 3.6 for the effective design widths vary quantitatively to a great extent. The differences are found mainly in the lower ranges of $\sqrt{f_{cr}/f_{max}}$. It may be explained by the shortcomings of the two assumptions used in the solutions.

For the purpose of comparison, von Karman's effective width formula (29), the modified Winter Formula (11), and the work of Hu, et al (31) are also shown in Figures 13 and 14. All studies indicate the same trend concerning the effect of initial curvature on the effective width of stiffened plates.

For Abdel-Sayed's two solutions, Equation 3.5 seems to agree favorably with the previous work in this area. However, as noted by Dawson

and Walker (36), Equation 3.5 gives an error of 5% for flat plates at $f_{max} = 5\ f_{cr}$, or $\sqrt{f_{cr}/f_{max}} = 0.448$; and 12% at $f_{max} = 9\ f_{cr}$, or $\sqrt{f_{cr}/f_{max}} = 0.342$. Dawson and Walker also pointed out that the percentage error can be neglected when $\sqrt{f_{cr}/f_{max}}$ exceeds 1.0.

From Figures 13 and 14, it can be seen that Equation 3.6 yields a much smaller effective width than Equation 3.5. In view of the fact that the work of Hu, et al has been considered to be the most accurate method, and that Equation 3.5 can provide results close to those of Hu, et al, Equation 3.5 may be considered as a better approximation for the actual case. The difference between Equations 3.5 and 3.6 can be attributed to the difference in deflection configurations assumed in the investigation.

A comparison of Figures 13 and 14 indicates that Winter's Formula tends to follow the solution by Equation 3.6. It allows for a larger initial curvature as the w/t increases. This observation is very important in considering the effects of initial curvature on the design of members cold-formed from thick sheets and plates.

Figures 15 and 16 show the correlation of the analytical and experimental results. These results are based on the studies conducted by Winter (15-17), Johnson and Winter (18), Sechler (16), Dwight and Ractliffe (36), and Wang and Errera (20). It can be seen that the experimental results generally agree with the formulas of von Karman and George Winter. It should be noted that Sechler's tests were carried out on disjointed single sheets, not on structural shapes. For this case, the imperfect edge conditions account for many low values in his tests (40).

IV. UNSTIFFENED COMPRESSION ELEMENTS

A. Statement of Problem

As mentioned previously, the study of initially curved plates is a very complex problem. Since an exact solution would be extremely difficult, an approximate solution seems to be dictated. One of the msot powerful approximate methods is the finite element technique, developed within the past ten to fifteen years. This type of mathematical idealization readily lends itself to a computer solution. This allows for less chance of mistakes and is quicker than the exact hand solutions. By increasing the number of elements, the desired accuracy can be obtained.

The unstiffened compression element is modeled as a rectangular plate simply supported on its loading edges and one longitudinal side. The other longitudinal side is a free edge. Figure 17 shows the idealized case. The plate considered is in uniaxial compression.

Timoshenko (21) uses a buckled shape which is described by the equation included in the literature review. Figure 18 illustrates the deflected shape assumed by Timoshenko. Both transverse and longitudinal curvatures exist in the buckled configuration. As was seen for stiffened elements, the transverse curvature as shown in Figure 2 tends to increase the buckling load; the longitudinal curvature as shown in Figure 1 tends to decrease the buckling load. For this reason, the intially curved plate was modeled for the longitudinal curvature only, without the consideration of the small amount of transverse curvature. This assumption should result in the minimum buckling

load, thus being conservative.

The deflected shape thus takes the form

$$\omega = f(y) \sin \frac{m\pi x}{a}$$

where $f(y) = A(\frac{a}{2} - y)$

a = the length of the plate

A = a constant, depending on the maximum deflection of the plate (at x = 0, y = w)

A rectangular mesh consisting of thirty-two elements was generated for the plate. The uniform compression load was modeled as concentrated loads at the nodal points. The size of the generated mesh is dependent upon the accuracy required, with due consideration given to allowable computer time. For this study, the 4 x 8 mesh gave sufficiently accurate results. Since the geometry and loadings of the plate were symmetrical about the y-axis only half the plate was needed for analysis, if the required boundary constraints are applied along the centerlines. Figure 19 shows the generated mesh for 16 elements.

The boundary conditions used in this finite element analysis were the same as those indicated by Timoshenko. Figure 20 illustrates the following symbols for rotations:

θ_x = rotation in the y-z plane about the x-axis

θ_y = rotation in the x-z plane about the y-axis

θ_z = rotation in the x-y plane about the z-axis

For this case the transverse edge follows the following boundary conditions:

$$\omega = 0,\ \theta_y = 0,\ \theta_z = 0,\ u = 0$$

The boundary conditions along the pinned longitudinal support are: $u=0$, $\omega=0$, $\theta_x=0$, and $\theta_z=0$. The boundary conditions along the centerline assuring continuity are:

$$u = 0,\ \theta_x = 0,\ v = 0$$

The longitudinal edge support does not restrict movement in the y-direction, but restrains buckling along this edge.

To develop a finite element program to solve this problem was considered to be too complex and beyond the scope of this study. Several available programs can be used to solve the buckling problem for this type of initially curved plate. A finite element program, NASTRAN, was used in this investigation. The following discussion describes the capabilities and liabilities of the NASTRAN program.

B. Method of Solution

NASTRAN is a multipurpose structural analysis computer program developed initially by NASA and modified by the Advanced Analytical Technology Department, at Ford Motor Company. Two major portions of the program, RIGID FORMAT #4 and #5, were utilized (38,39). Both formats were developed to assist the design of automotive components and systems.

RIGID FORMAT #5 is used to determine critical buckling loads and cooresponding mode shapes of structural components. These components

when compressed axially with loads below the critical value remain straight in stable equilibrium. Under stable equilibrium, a small disturbance will cause small displacements. After removal of the load, the structure will return to its original state. When the compressive axial load exceeds a limiting value, it becomes unstable. Any lateral disturbance will cause large deflection and the structure will not return to its previous state, upon removal of the disturbance. The structure may be in unstable equilibrium with discrete values of axial load. The critical load is the smallest of these loads. These different loads occur at the different buckled mode shapes of the structure. RIGID FORMAT #5 performs an eigenvalue analysis to find these unstable mode shapes. The critical load is dependent on the material, geometry of the structure, and support conditions.

The major liability with RIGID FORMAT #5, as already hinted at, is its restriction to perfectly straight beams or flat plates. Lateral forces, moments, or eccentricities cannot be handled. If the resulting buckling load from RIGID FORMAT #5 is less than the applied load, the result is valid. If the resulting buckling load is larger than the applied load, buckling may not have occurred. The effect of deflections may become important in the buckling strength of the system. Just as membrane stresses increase the buckline strength, a non-linear stiffness matrix could result, depending on deflections. In the case analysis by the Differential Stiffness Approach, RIGID FORMAT #4 is required.

When the structure to be analyzed already has a lateral deflected shape, the RIGID FORMAT #5 will not give accurate results. These

lateral deflections may be the result of existing lateral forces or initial curvature. An incremental stiffness, referred to as "differential stiffness" is needed to express the difference in lateral stiffness due to the large lateral deformations already in existance. This initial deflection will cause the p-Δ effect to become noticeable and reduce the buckling load of the structure.

Because the structure already has initial lateral deflections as the compressive load is applied, further lateral deflections take place. When the compressive load is increased, the lateral deflection increases more rapidly because the p-Δ effect progressively affect the shape of the structure. Thus, instead of staying in the original shape until unstable equilibrium is reached as in the case of the flat members, the lateral deflection of the structure gradually increases until an overwhelming increase in lateral deflection is caused by a very little increase in load. When this state occurs, by definition, the buckling load is said to have been reached.

RIGID FORMAT #4 uses a Differential Stiffness Approach to arrive at the buckling load for initially curved members, eccentric loadings, or combination lateral and compressive loadings. A series of load levels are run with the deflections as output. By plotting the load-deflection curves the buckling load can be found.

RIGID FORMAT #4 has a program limitation that a lateral deflected shape has to exist. As stated before, this can result from various conditions. Thus, RIGID FORMAT #5 was used to handle the flat plate cases using the eigenvalue analysis to predict the buckling load.

RIGID FORMAT #4 was used to analyze the initially curved plates, using load-deflection curves to predict the buckling load.

C. Presentation of Results

As stated previously, different degrees of initial deviation from flatness were studied in this investigation. Because this study is mostly concerned with thin-walled material, a w/t ratio of 30 was used. By using this selected ratio of w/t, the buckling stress of the plate was obtained before stresses reached the plastic range. Dimensions of the plate and the generated mesh are shown in Figure 19. The modulus of elasticity was taken as 29,500 ksi and Poisson's ratio was 0.3. The deflected shape is represented by Equation 4.1:

$$\omega_o = f_o(y) \sin \frac{m\pi x}{a} \tag{4.1}$$

where $f_o(y) = A_o(\frac{a}{2} - y)$

For this study, initial deviations (δ_o/t) of 0.0, 0.1, 0.2, 0.3, 0.5 were considered for length-to-width ratios (a/w) of 2 and 4. The coordinates of the nodal points conform to Equation 4.1, as given in Table II. Table III contains the z-coordinates for the initially curved plate used for a/w = 2 and 4.

RIGID FORMAT #5 was used for the two flat cases. Resultant eigenvalues are presented in Table IV for the given load level of 14,800 pounds. The buckling load is defined as the applied load multiplied by the critical eigenvalue (i.e. the smallest). For a flat plate with a/w = 2, the resultant buckling load was 24,600 pounds.

Timoshenko (21) gave a value of 24,789.65 pounds for the theoretical buckling load. The finite element result is only 0.6% smaller than the theoretical load. For a plate with a/w = 4 the resultant buckling load was 17,519.92 pounds. Timoshenko gave a value of 18,325.82 pounds. In this case, the finite element result is only 4.39% smaller than the theoretical value. These values are well within the allowable accuracy for this study.

NASTRAN RIGID FORMAT #4 allows for input of loads on the structure with optional load factors. The initially curved plates were run with a load base of 4000 pounds with various load factors to cover the desired range of deflection. Results obtained from the RIGID FORMAT #4 for eight different cases are presented in Tables V and VI. The applied load was obtained by multiplying the load base by the load factor. The load deflection curves are shown in Figure 21 for the results of six cases studied for a/w = 2 and 4.

The top-of-the-knee method as described in Reference 31 was used to define the buckling load of the initially curved elements. The buckling load is defined as the transition stage from low to high rate of increase in lateral deflection with load. As can readily be seen, this type of approach depends greatly on the personal judgement of the one evaluating the results.

Figure 21 shows the critical buckling loads determined by the author. With the small amount of curvature that exists in these results, a different level may be chosen by others. Table VII presents the selected buckling load for each case.

As seen previously for the stiffened plates, the unstiffened plates show a decrease in buckling load as the degree of initial curvature increases. The most influential point is around the buckling load. As the load exceeds the critical buckling load, the initial deviation has less effect.

It should also be noted that for the same δ_o/t ratio, the buckling stress of the unstiffened element reduces more percentage-wise than that for the stiffened element. This is possibly due to the difference in magnitude of the buckling stress for the different types of flat plates. Because the membrane stress tends to contribute less to the structural integrity of the unstiffened element, this type of element is affected more by the initial curvature as compared with the stiffened elements.

V. CONCLUSIONS AND RECOMMENDATIONS

A. Comparison of Results

A comprehensive study of the effect of initial deviation from flatness on the effective design width of stiffened elements and on the buckling stress for unstiffened elements was presented. For both stiffened and unstiffened elements, considerations were given to the initial deviations of δ_o/t = 0, 0.1, 0.2, 0.3, 0.5, 0.7, and 1.0.

Previous research work and the further study carried out in this investigation indicated that initial deviations tend to decrease the buckling stress and post-buckling strength of the structural components. The most noticeable influence on initial deviation was found to be around the above or below this load level.

B. Impact on Design Criteria

Two observations in particular have been noted by the author. First is the question of correlating the presented results to actual initial deviations from flatness found in standard cold-forming practices. As stated previously, to obtain the practical tolerances for this type of product is difficult. One indication of such tolerances for this type of structural members might be found in the ASTM Specifications for production of plate, sheet, and strip steel. In general, the initial deviation to thickness ratio (δ_o/t) tends to decrease as the base metal thickness increases.

The second observation is that this initial deviation from flatness may have more bearing on design requirements for unstiffened plates than for stiffened plates. This is because the unstiffened plates

are usually designed for the initial buckling stress, for which the effect of initial deviation on the reduction of buckling load is more pronounced. For stiffened compression element, the effect of the initial deviation on the load-carrying capacity of the element is based on the effective width determined for the initially curved plate.

C. Recommendations

The correlation of the base metal thickness with initial deviations from flatness would provide enough information to determine whether the present design requirements are adequate or too conservative for the thicker base metals. In view of the fact that thick sheets and plates usually have small δ_o/t ratios as compared with thin sheets, the present AISI design formulas for determining the effective design width of stiffened elements and the allowable stress for unstiffened elements can be conservatively used for sections cold-formed from thick sheets and plates.

BIBLIOGRAPHY

1. American Iron and Steel Institute, Specification for the Design of Cold-Formed Steel Structural Members, 1968 Edition.

2. American Iron and Steel Institute, "Addendum No. 1 to Specification for the Design of Cold-Formed Steel Structural Members," November 19, 1970.

3. "Standard Specification for Flat-Rolled Carbon Steel Sheets of Structural Quality," ASTM Designation A245-64.

4. "Standard Specification for High-Strength Low-Alloy Cold-Rolled Steel Sheets and Strip," ASTM Designation A374-68.

5. "Standard Specification for High-Strength Low-Alloy Hot-Rolled Steel Sheets and Strip," ASTM Designation A375-64.

6. "Standard Specification for Zinc-Coated (Galvanized) Steel Sheets of Structural Quality, Coils and Cut Lengths," ASTM Designation A446-69.

7. "Standard Specification for Hot-Rolled Carbon Steel Sheets and Strip, Structural Quality," ASTM Designation A570-70.

8. "Standard Specification for Steel Sheets and Strip, Hot-Rolled and Cold-Rolled, High Strength, Low-Alloy with Time Proven Corrosion Resistance," ASTM Designation A606-70.

9. "Standard Specification for Steel Sheet and Strip, Hot-Rolled and Cold-Rolled, High Strength, Low-Alloy Columbium and/or Vanadium," ASTM Designation A607-70.

10. "Standard Specification for Steel, Cold-Rolled, Sheet, Carbon, Structural Quality," ASTM Designation A611-70.

11. Winter, G., Commentary on the 1968 Edition of the Specification for the Design of Cold-Formed Steel Structural Members, published by American Iron and Steel Institute, 1970.

12. Rolf, S.T., Discussion of "Effect of Cold-Work in Cold-Forming Steel Structural Members," Cornell Engineering Research Bulletin, 70-1, p. 37.

13. Kirkland, William G., "Cold-Roll Forming Practice in the United States," American Iron and Steel Institute, Revised, April 1966.

14. American Institute of Steel Construction, Manual of Steel Construction, Seventh Edition, 1970.

15. Winter, G., "Strength of Thin Steel Compression Flanges," ASCE Transactions, Paper #2305, Vol. 112, 1947.

16. Winter, G., "Strength of Thin Steel Compression Flanges," Cornell University Engineering Experiment Station, Bull. No. 35/3, October 1947.

17. Winter, G., "Performance of Thin Steel Compression Flanges," Cornell University Engineering Experiment Station, Bull. No. 33, November 1, 1950.

18. Johnson, A.L., and Winter, G., "Behavior of Stainless Steel Columns and Beams," ASCE Proceedings, Journal of Structural Division, Vol. 92, No. ST5, October 1966.

19. Dwight, J.B., and Ractliffe, A.T., "The Strength of Thin Plates in Compression," Thin Walled Structures, Gordon and Breach Science Publishers, 1968.

20. Wang, S.T., and Errera, S.J., "Behavior of Cold-Rolled Stainless Steel Members," Proceedings of the First Specialty Conference on Cold-Formed Steel Structures, University of Missouri-Rolla, August 1971.

21. Timoshenko, S.P., and Gere, J.M., Theory of Elastic Stability, McGraw-Hill Book Company, New York, 1961.

22. Bulson, P.S., The Stability of Flat Plates, American Elsevier Publishing Company, Inc., New York, 1969.

23. Saint Venant, "Discussion in Theorre de l'elasticite' des Corps Solides," by Clebsch, p. 704, 1883.

24. Von Karman, T., "Festigkeitsprobleme in Maschinenbau," Encyklpadie der Mathematischen, Vol. 4, 1910, p. 349.

25. Schnadel, G., "Die Uberschreitung der Knickgrenze bei dunnen Platten," Proceedings of the Third International Congress for Applied Mechanics, Stockholm, Vol. 3, 1930, pp. 73-81.

26. Cox, H.L., "The Buckling of Thin Plates in Compression," Technical Report of the Aeronautical Committee, 1933-34, pp. 443-463.

27. Marguerre, K., "Die mittragende Breite der gedrucklen Platte," Luftfahrtforschung, Vol. 14, 1937, pp. 121-128.

28. Levy, S., "Bending of Rectangular Plates with Large Deflections," NACA TR-737, 1942.

29. Von Karman, T., Schler, E.E., and Donnell, L.H., "The Strength of Thin Plates in Compression," ASME Transactions, APM-54-5 Vol. 54, No. 2, January 30, 1932, p. 53.

30. Marguerre, K., "Zur Theorie der gekrummlen Platte grosser Formanderung," Proceedings of the Fifth International Congress for Applied Mechanics, Cambridge, 1938, pp. 93-101.

31. Hu, P.C., Lundquist, E., and Batdorf, S.B., "Effect of Small Deviation from Flatness on the Effective Width and Buckling of Plates in Compression," NACA TN No. 1124, 1946.

32. Coan, J.M., "Large-Deflection Theory for Plates with Small Initial Curvature Loaded in Edge Compression," ASME Transactions, Journal of Applied Mechanics, Vol. 73, 1951, p. 143.

33. Yamaki, N., "Postbuckling Behavior of Rectangular Plates with Small Initial Curvature Loaded in Edge Compression," ASME Journal of Applied Mechanics, September 1959, p. 407.

34. Abdel-Sayed, George, "Effective Wdith of Thin Plates in Compression," ASCE Proceedings, Journal of Structural Division, October, 1969.

35. Yang, T.Y., "Non-linear Buckling of Thin-Walled Components," Proceedings of the First Specialty Conference on Cold-Formed Steel Structures, University of Missouri-Rolla, August 1971.

36. Dawson, Ralph G., and Walker, Alastair C., "Post-Buckling of Geometrically Imperfect Plates," ASCE Proceedings, Journal of Structural Division, Vol. 98, ST1, January 1972, p. 75.

37. Bruhn, E.E., Analysis and Design of Flight Vehicle Structures, Tri-state Offset Company, Cincinnati, Ohio, 1965.

38. Conklu, O., "Static Analysis with Differential Stiffness, Rigid Format 4," Ford Engineering Evaluation and Materials Office, Product Planning and Research Staff, Report No. 1278E-2, June 30, 1972.

39. Conklu, O., "Buckling, Rigid Format 5," Ford Engineering Evaluation and Materials Office, Product Planning and Research Staff, Report No. 1278E-1, June 30, 1972.

40. Yu, W.W., Cold-Formed Steel Structures, McGraw-Hill Book Company, New York, 1973.

41. Buchert, K.P., "Buckling of Curved Flange Shell-Like Columns," presented at the Technical Session of the Column Research Council, Houston, Texas, March 27, 1974.

VITA

William Morris McKinney was born on August 6, 1949 in St. Louis, Missouri, the son of Mr. and Mrs. Herman M. McKinney. He received his primary education at Hope Lutheran School in St. Louis, Missouri. He received his secondary education at Lutheran High School South in Affton, Missouri. In September, 1967 he entered the University of Missouri-Rolla and graduated in May, 1971 with a Bachelor of Science Degree in Civil Engineering. During his last semester as an undergraduate he was dually enrolled and took both graduate and undergraduate courses. In August, 1971 he entered Graduate School at the University of Missouri-Rolla. He held a graduate research assistantship in the Civil Engineering Department from that time till May, 1972.

He worked for J. Ray McDermott, Inc. as a design engineer from June, 1972 to January 1973. He has worked at Southwest Research Institute since February, 1973 as a Marine and Structural Engineer.

He is a member of the American Society of Civil Engineers. He is also a member of Phi Eta Sigma, Chi Epsilon, Tau Beta Pi, Phi Kappa Phi, and Theta Xi, all honorary societies.

APPENDICES

APPENDIX A

Notations

α constant, $\sqrt{\frac{m^2\pi^2}{a^2} + \sqrt{\frac{\sigma_x t}{D} \cdot \frac{m^2\pi^2}{a^2}}}$

β constant, $\sqrt{-\frac{m^2\pi^2}{a^2} + \sqrt{\frac{\sigma_x t}{D} \cdot \frac{m^2\pi^2}{a^2}}}$

δ lateral deflection of a plate

δ_o initial lateral deflection of a plate

$\bar{\varepsilon}_a$ the unit plate shortening in the x-direction

ε_{cr_x} the critical strain in the x-direction for a flat plate subjected to a compressive stress in the x-direction

$\varepsilon_x, \varepsilon_y, \varepsilon_z$ unit strains in x, y, and z directions

$\theta_x, \theta_y, \theta_z$ rotation about the x, y, and z axes

μ Poisson's Ratio

$\bar{\sigma}_a$ the average edge compression in the x-direction

σ_{cr} critical buckling stress

σ_{cr_x} the critical stress of the flat plate

$\sigma_x, \sigma_y, \sigma_z$ unit normal stresses on planes perpendicular to the x, y, and z axes

$\tau_{xy}, \tau_{yz}, \tau_{xz}$ unit shear stresses on planes perpendicular to the x, y, and z axes and parallel to the y, z, and x axes

ϕ the aspect ratio of the plate a/w and a constant

ω the lateral deflection of the plate, deflection in the z direction

ω_o the initial deflection in the z direction

$\omega_{o_{mn}}$ the amplitude of a trigonometric function defining the initial lateral deflection of a plate

A, A_1, A_2, A_3, A_4 constant

a the length of the plate

a_{mn} the amplitude of a trigonometric function

B constant

b width or effective design width for plate subjected to buckling

c constant, $\frac{\pi}{\sqrt{3(1-\mu^2)}}$

C_1, C_2, C_3, C_4 constants

D the plate flexural rigidity, $Et^3/12(1-\mu^2)$

D_x, D_y, D_z the first derivative with respect to x, y, z

e the net deflection in the z-direction

e_o the initial deflection in the z-direction

E Modulus of Elasticity

$f(y), f$ a function of y alone

f_{max} maximum stress

K buckling coefficient

k load level

k_o δ_o/t

M constant

M_x, M_y, M_z moments about the x, y, and z axes

m, n number of waves in the deflected shape in the x and y directions

N_a average loading per unit length in x - y plane

N_{cr} the critical buckling load

$(\bar{n}_y)$ the average loading per unit length in the y-direction

$(n_y)_{max}$ the maximum loading per unit length in the y-direction

N constant

p constant, $[\frac{m\pi}{\phi}^2 (\sqrt{k} + \frac{m}{\phi})]^{1/2}$

P_{ult} ultimate load

q a uniform load applied to the plate

q_1 constant, $[\frac{m\pi}{\phi}^2 (\sqrt{k} - \frac{m}{\phi})]^{1/2}$

r radius of curvature

r_1 constant, $\sqrt{p^2 - \mu \frac{m^2\pi^2}{\phi^2}}$

s constant, $\sqrt{q_1^2 + \mu \frac{m^2\pi^2}{\phi^2}}$

t thickness of the plate

u displacement in x-direction

v displacement in y-direction

w width of plate

x,y,z rectangular coordinates

APPENDIX B

Tables

Table I(A) Effective Widths for Initially Curved Stiffened Elements (Equation 3.5)

δ_o/t	w/t	b/t	$\sqrt{f_{cr}/f_{max}}$
0.0	37.4	37.3	2.232
	53.0	52.8	1.577
	70.4	69.8	1.186
	91.9	83.1	0.909
	115.2	89.1	0.725
	136.3	93.9	0.613
	154.8	98.3	0.540
	179.2	104.6	0.467
	200.8	110.7	0.416
0.1	37.7	37.3	2.215
	53.6	52.9	1.558
	72.8	69.7	1.147
	88.4	78.7	0.746
	119.6	88.3	0.699
	139.3	93.2	0.600
	157.0	97.9	0.530
	180.8	104.3	0.462
	201.9	110.4	0.414
0.2	38.7	37.3	2.158
	55.7	52.8	1.499
	70.6	64.4	1.183
	87.0	73.8	0.961
	115.8	84.3	0.721
	134.8	89.7	0.620
	152.3	94.7	0.548
	183.0	103.7	0.457
	197.1	107.9	0.424
0.3	40.2	37.2	2.077
	67.0	58.5	1.247
	93.0	72.9	0.898
	121.1	83.2	0.690
	139.0	88.8	0.601
	155.8	93.8	0.537
	178.0	101.0	0.470
	198.8	107.5	0.420

Table I(A) Effective Widths for Initially Curved Stiffened Elements (Equation 3.5)(Continued)

δ_o/t	w/t	b/t	$\sqrt{f_{cr}/f_{max}}$
0.5	44.1	36.8	1.894
	55.2	44.9	1.515
	74.7	57.4	1.119
	93.4	67.0	0.895
	120.6	78.2	0.695
	137.8	84.3	0.607
	154.0	89.8	0.543
	181.8	100.1	0.460
	201.6	106.6	0.415
0.7	33.4	25.7	2.500
	60.3	44.0	1.385
	71.2	50.5	1.173
	91.2	61.0	0.917
	118.6	73.2	0.705
	135.6	79.7	0.616
	159.3	88.5	0.525
	180.9	96.2	0.462
	197.5	104.0	0.423
1.0	37.3	24.8	2.238
	53.7	35.0	1.556
	66.9	42.6	1.249
	89.2	54.4	0.937
	117.7	67.5	0.710
	134.8	74.8	0.620
	158.2	84.1	0.528
	179.6	92.3	0.465
	200.2	103.4	0.418

Table I(B) Effective Widths for Initially Curved Stiffened Elements (Equation 3.6)

δ_o/t	w/t	b/t	$\sqrt{f_{cr}/f_{max}}$
0.0	37.4	37.3	2.232
	53.0	52.7	1.577
	70.4	69.4	1.186
	91.9	76.0	0.909
	115.2	72.7	0.725
	136.3	71.8	0.613
	154.8	72.2	0.540
	179.2	74.1	0.467
	200.8	76.6	0.416
0.1	37.7	37.0	2.215
	53.6	52.1	1.558
	72.8	67.1	1.147
	88.4	71.2	0.746
	119.6	70.1	0.699
	139.3	70.2	0.600
	157.0	71.2	0.530
	180.8	73.4	0.462
	201.9	76.1	0.414
0.2	38.7	36.1	2.158
	55.7	50.1	1.499
	70.6	59.4	1.183
	87.0	64.2	0.961
	115.8	66.4	0.721
	134.8	67.4	0.620
	152.3	68.8	0.548
	183.0	72.5	0.457
	197.1	74.5	0.424
0.3	40.2	34.7	2.077
	67.0	52.1	1.247
	93.0	60.1	0.898
	121.1	63.4	0.690
	139.0	65.4	0.601
	155.8	67.3	0.537
	178.0	70.6	0.470
	198.8	73.8	0.420

Table I(B) Effective Widths for Initially Curved Stiffened Elements (Equation 3.6)(Continued)

δ_o/t	w/t	b/t	$\sqrt{f_{cr}/f_{max}}$
0.5	44.1	31.6	1.894
	55.2	38.0	1.515
	74.7	46.7	1.119
	93.4	52.3	0.895
	120.6	58.0	0.695
	137.8	60.9	0.607
	154.0	63.5	0.543
	181.8	69.2	0.460
	201.6	72.8	0.415
0.7	33.4	20.9	2.500
	60.3	34.7	1.385
	71.2	39.3	1.173
	91.2	46.0	0.917
	118.6	53.0	0.705
	135.6	56.7	0.616
	159.3	61.4	0.525
	180.9	65.7	0.462
	197.5	70.8	0.423
1.0	37.3	18.7	2.238
	53.7	26.0	1.556
	66.9	31.3	1.249
	89.2	39.2	0.937
	117.7	47.5	0.710
	134.8	51.8	0.620
	158.2	57.4	0.528
	179.6	62.3	0.465
	200.2	69.8	0.418

Table II. Coordinates of Flat Unstiffened Element**

Nodal Point	X Coordinate a/w=2	X Coordinate a/w=4	Y Coordinate	Initial Deflection*
1	0.	0.	0.	0.0
2	1.5	3.0	0.	0.0
3	3.0	6.0	0.	0.0
4	4.5	9.0	0.	0.0
5	6.0	12.0	0.	0.0
6	0.	0.0	1.5	.25 A_o
7	1.5	3.0	1.5	.23097 A_o
8	3.0	6.0	1.5	.17678 A_o
9	4.5	9.0	1.5	.09567 A_o
10	6.0	12.0	1.5	0.0
11	0.	0.0	3.0	.50 A_o
12	1.5	3.0	3.0	.46194 A_o
13	3.0	6.0	3.0	.35356 A_o
14	4.5	9.0	3.0	.19134 A_o
15	6.0	12.0	3.0	0.0
16	0.	0.0	4.5	.75 A_o
17	1.5	3.0	4.5	.69291 A_o
18	3.0	6.0	4.5	.53033 A_o
19	4.5	9.0	4.5	.28701 A_o
20	6.0	12.0	4.5	0.0
21	0.	0.0	6.0	1.0 A_o
22	1.5	3.0	6.0	.92388 A_o
23	3.0	6.0	6.0	.70711 A_o
24	4.5	9.0	6.0	.38268 A_o
25	6.0	12.0	6.0	0.0

*Initial deflection, ω_o, is the coefficient x A_o. Refer to Fig. 19
**All dimensions in inches.

Table III. Z-Coordinates of Initially Curved Elements (a/w = 2 and 4)*

Nodal #	k_o				
	0.1	0.2	0.3	0.4	0.5
1	0.0	0.0	0.0	0.0	0.0
2	0.0	0.0	0.0	0.0	0.0
3	0.0	0.0	0.0	0.0	0.0
4	0.0	0.0	0.0	0.0	0.0
5	0.0	0.0	0.0	0.0	0.0
6	0.0050	.0100	.0150	.0200	.0250
7	0.0046	.0092	.0138	.0184	.0231
8	0.0035	.0070	.0106	.0141	.0176
9	0.0019	.0038	.0057	.0076	.0956
10	0.0	0.0	0.0	0.0	0.0
11	0.0100	.0200	.0300	.0400	.0500
12	0.0092	.0184	.0276	.0368	.0460
13	0.0070	.0141	.0212	.0282	.0352
14	0.0038	.0076	.0114	.0152	.0191
15	0.0	0.0	0.0	0.0	0.0
16	0.150	.0300	.0450	.0600	.0750
17	0.136	.0277	.0416	.0543	.0693
18	0.106	.0212	.0318	.0424	.0530
19	0.0057	.0115	.0172	.0230	.0287
20	0.0	0.0	0.0	0.0	0.0
21	0.02	.0400	.0600	.0800	.1000
22	0.0185	.0370	.0554	.0739	.0984
23	0.0141	.0283	.0424	.0566	.0707
24	0.0076	.0153	.0229	.0306	.0383
25	0.0	0.0	0.0	0.0	0.0

*All dimensions in inches.

Table IV. Eigenvalues for Flat Compression Elements

a/w	Eigenvalue	Load Level (lbs.)	Buckling Level (lbs.)
2	1.664900	14,800	24,600
4	1.183779	14,800	17,550

Table V. Lateral Deflections for Unstiffened Elements (a/w = 2.0)

Load Factor*	Load (lbs.)	Center Deflection (in.)			
		k_o=0.1	k_o=0.2	k_o=0.3	k_o=0.5
2.0	8,000	0.0093	0.0186	0.074	0.0437
4.0	16,000	0.058	0.0704	0.1023	0.1551
5.0	20,000	0.0827	0.1598	0.2257	0.3179
5.2	20,800	--	--	0.2771	--
5.4	21,600	--	--	0.3513	--
5.5	22,000	0.1581	0.2969	--	0.5151
5.6	22,400	--	--	0.4677	--
5.8	23,200	--	--	0.6763	--
6.0	24,000	--	--	1.1594	--
6.1	24,400	--	--	1.7558	--
6.2	24,800	--	--	5.6844	--
6.4	25,600	--	--	-3.9207	--

*Load base is 4,000 lbs.

Table VI. Lateral Deflections for Unstiffened Elements (a/w = 4.0)

Load Factor*	Load (lbs.)	Center Deflection (in.)			
		k_o=0.1	k_o=0.2	k_o=0.3	k_o=0.5
2.0	8,000	0.0163	0.0325	0.0480	0.0760
3.0	12,000	0.0421	0.0830	0.1208	0.1939
4.0	16,000	0.2001	0.3745	0.5049	0.6374

*Load base is 4,000 lbs.

Table VII. Buckling Load of Unstiffened Elements Based on the Top-of-the-Knee Method

a/w	k_o	Buckling Load (lbs)
2.0	0.0	24,640
	0.3	19,500
	0.5	16,900
4.0	0.0	17,519
	0.3	13,750
	0.5	10,600

APPENDIX C

Figures

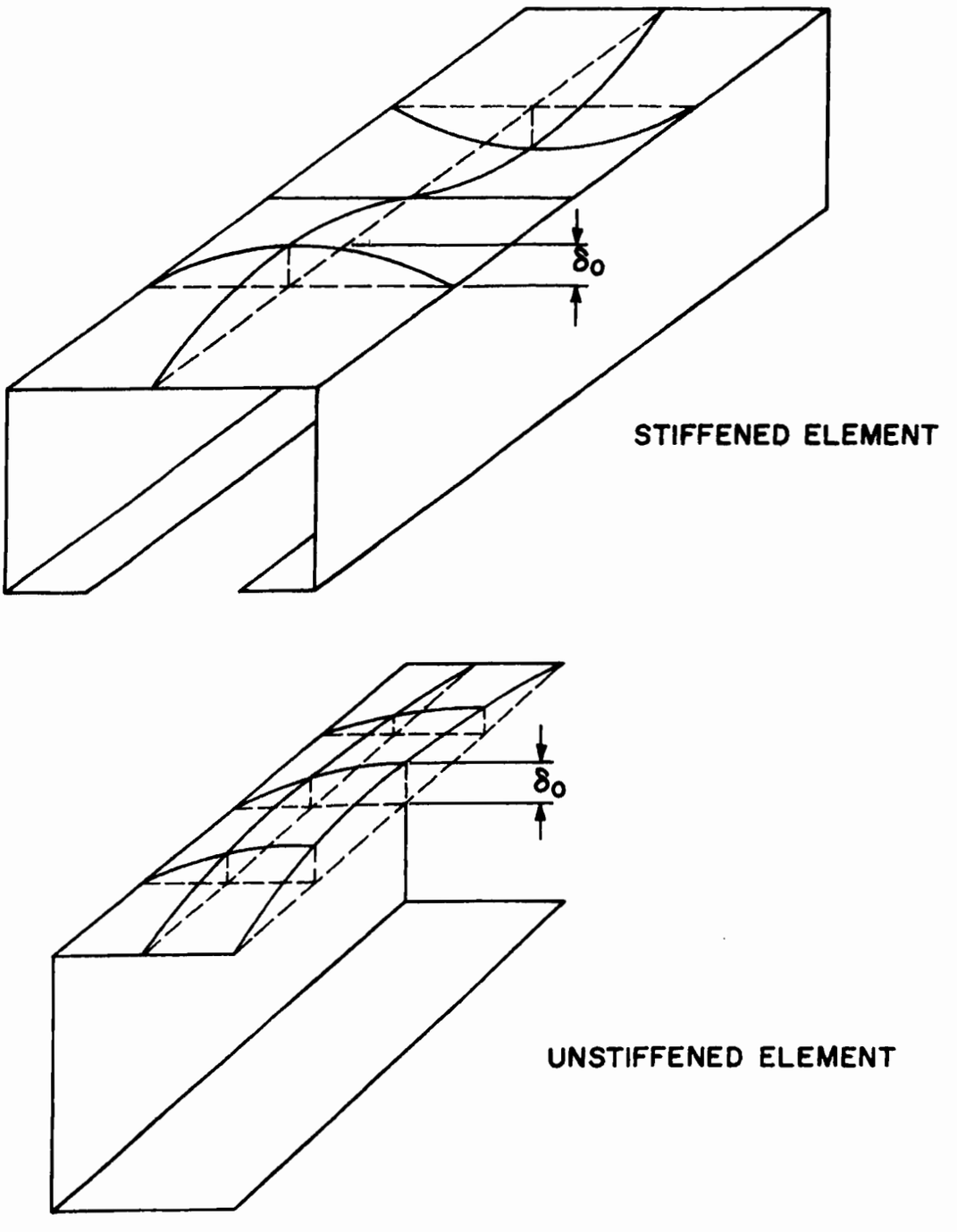

Figure 1. Longitudinal Initial Curvature

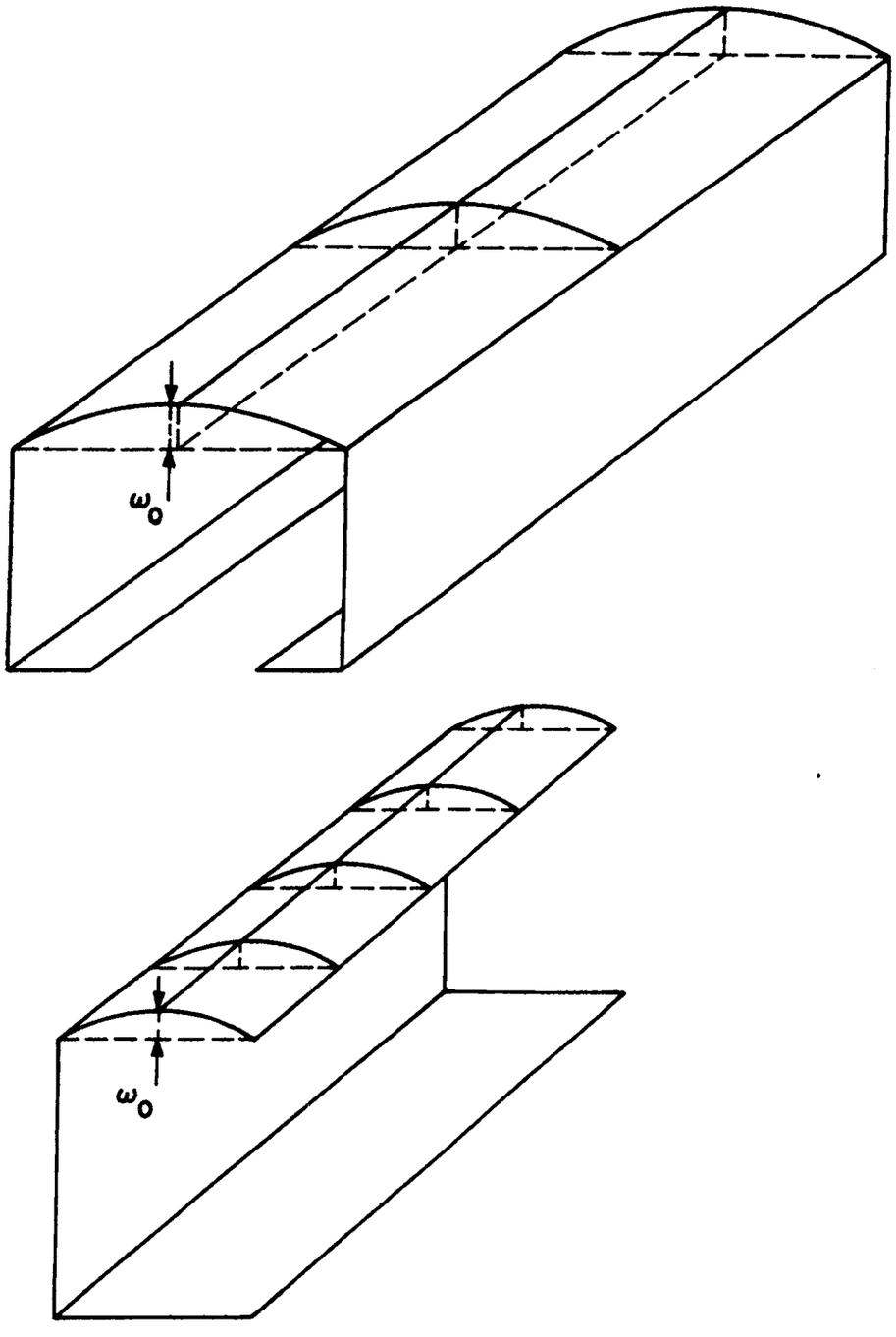

Figure 2. Transverse Initial Curvature

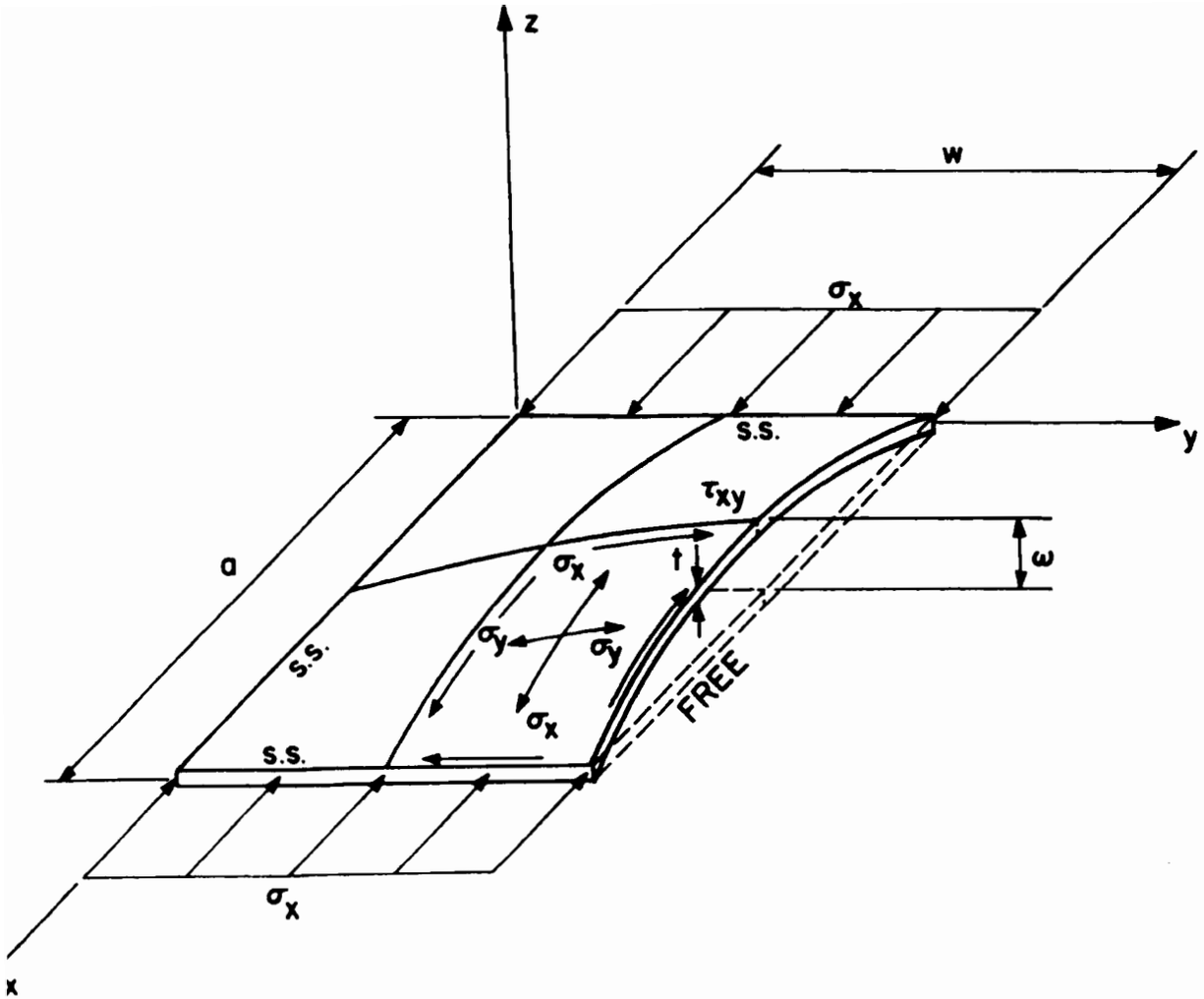

Figure 3. Coordinates and Stress Components of Unstiffened Element

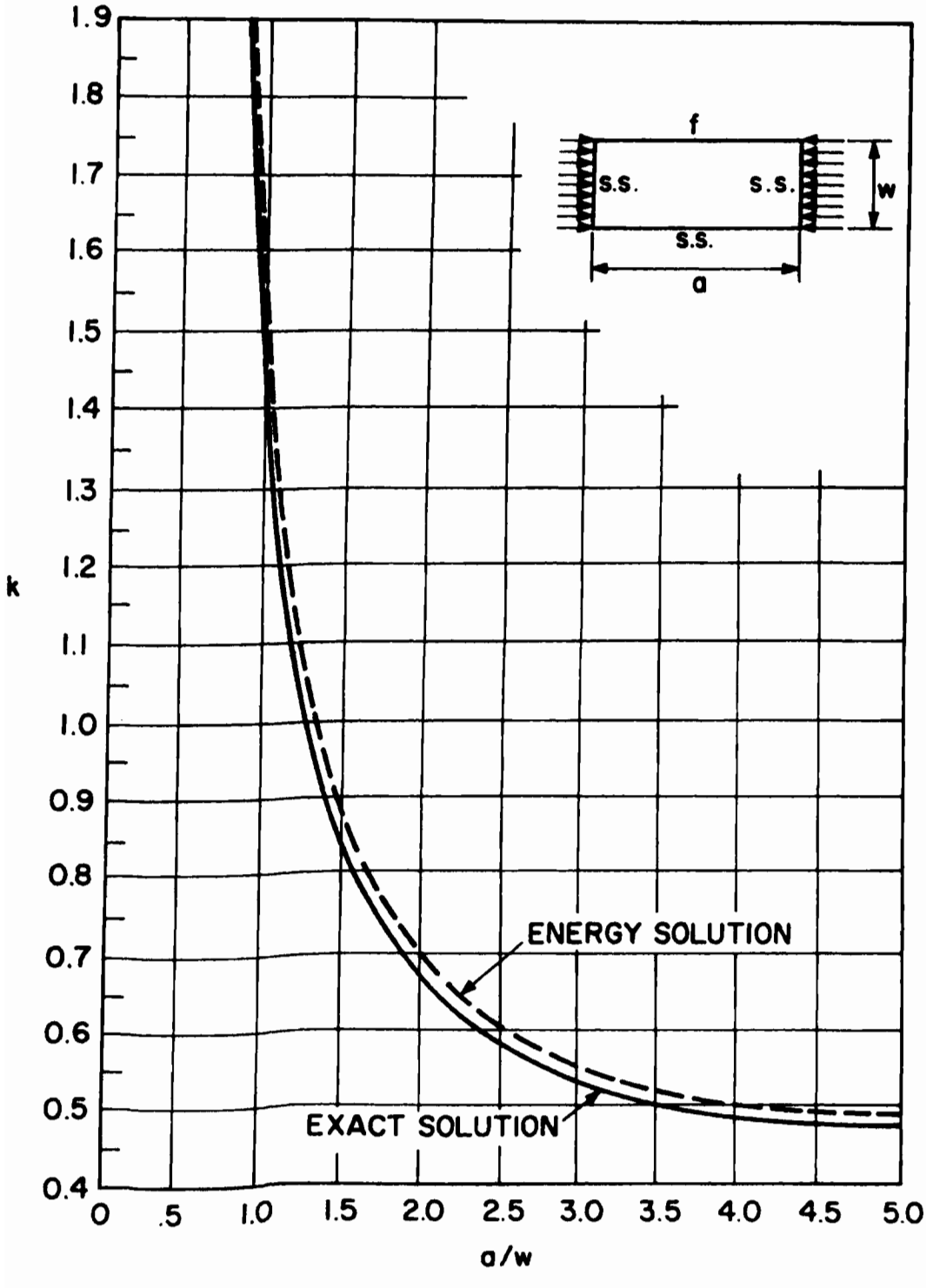

Figure 4. Buckling Coefficient for Flat Unstiffened Elements

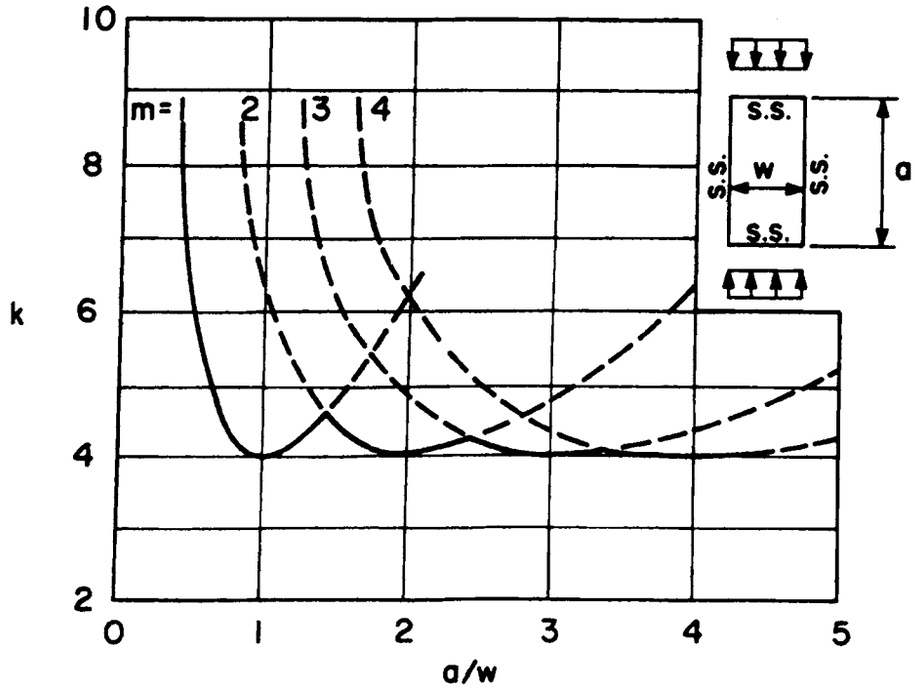

Figure 5. Buckling Coefficient for Flat Stiffened Elements

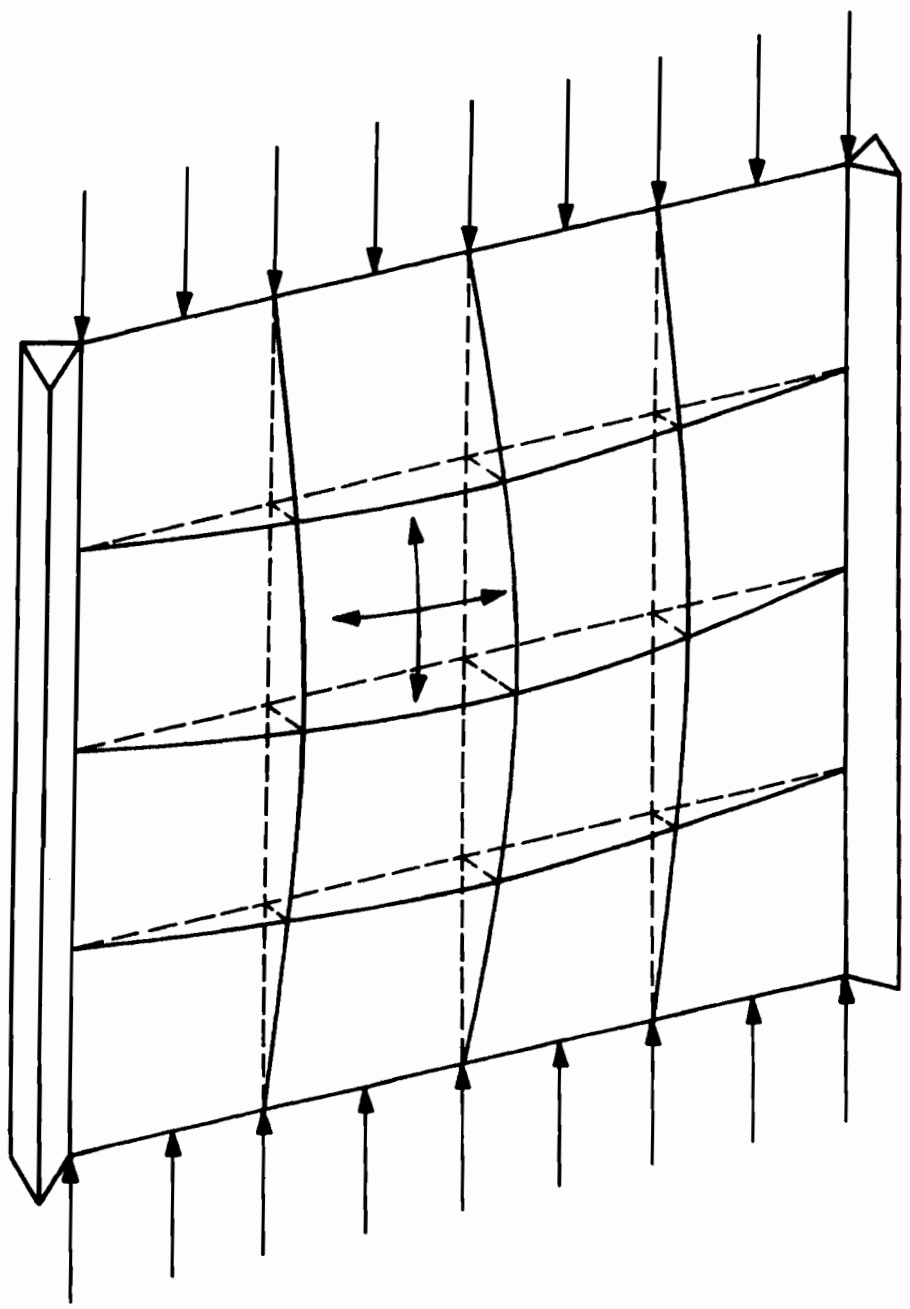

Figure 6. Stiffened Element in Post-Buckling Range

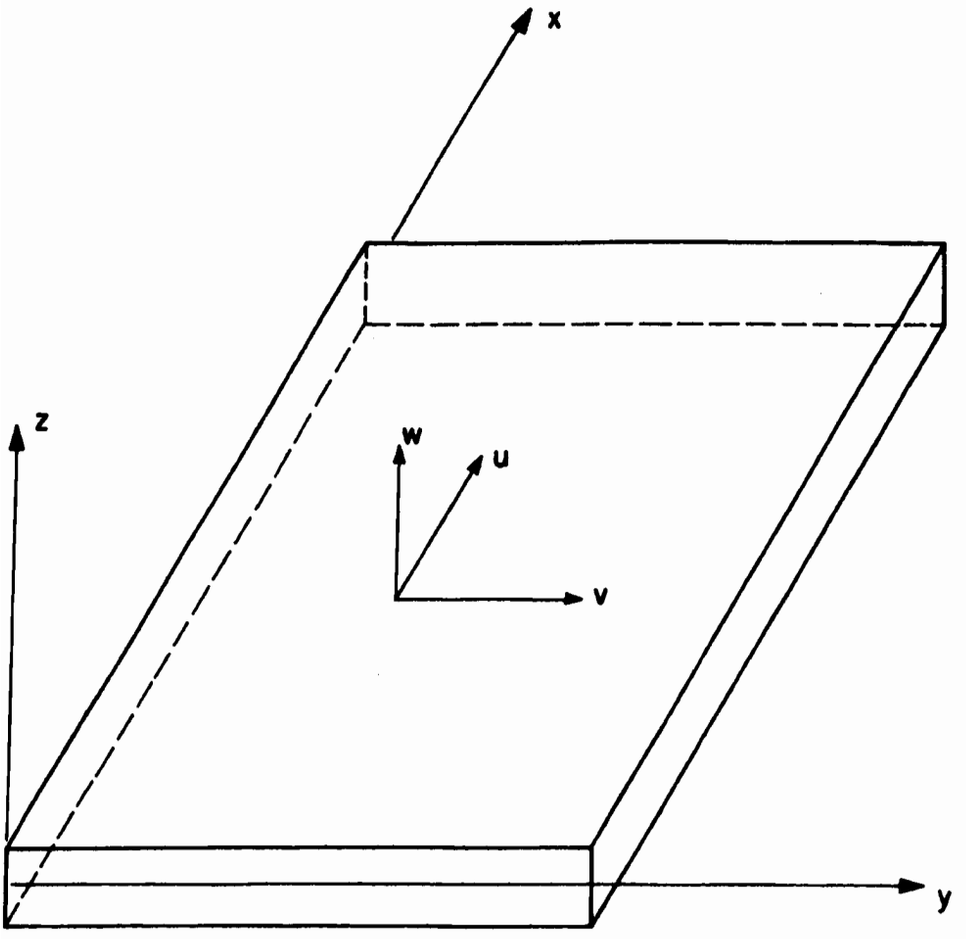

Figure 7. Local Coordinate System

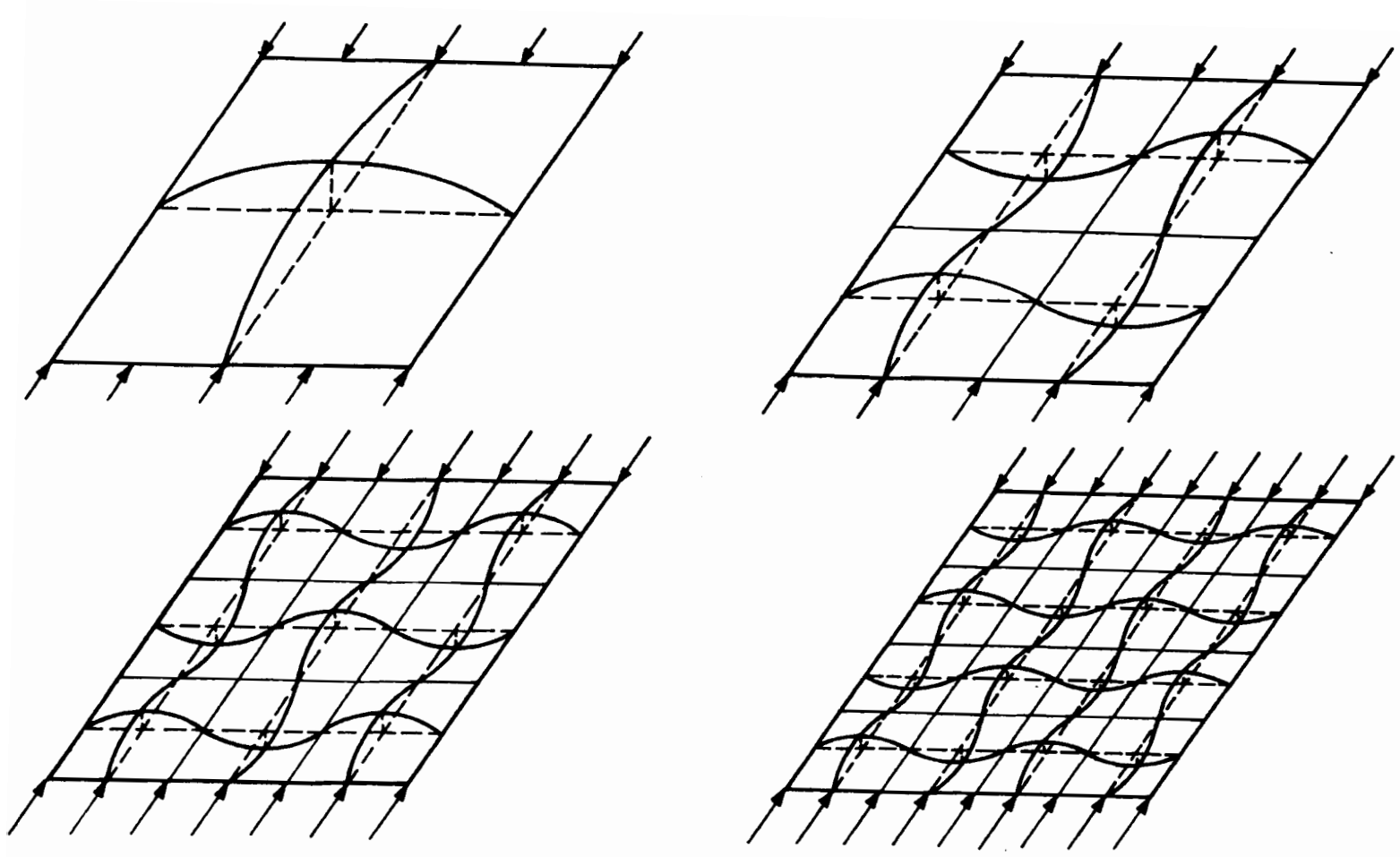

Figure 8. Deflected Configurations for Simply Supported Plates

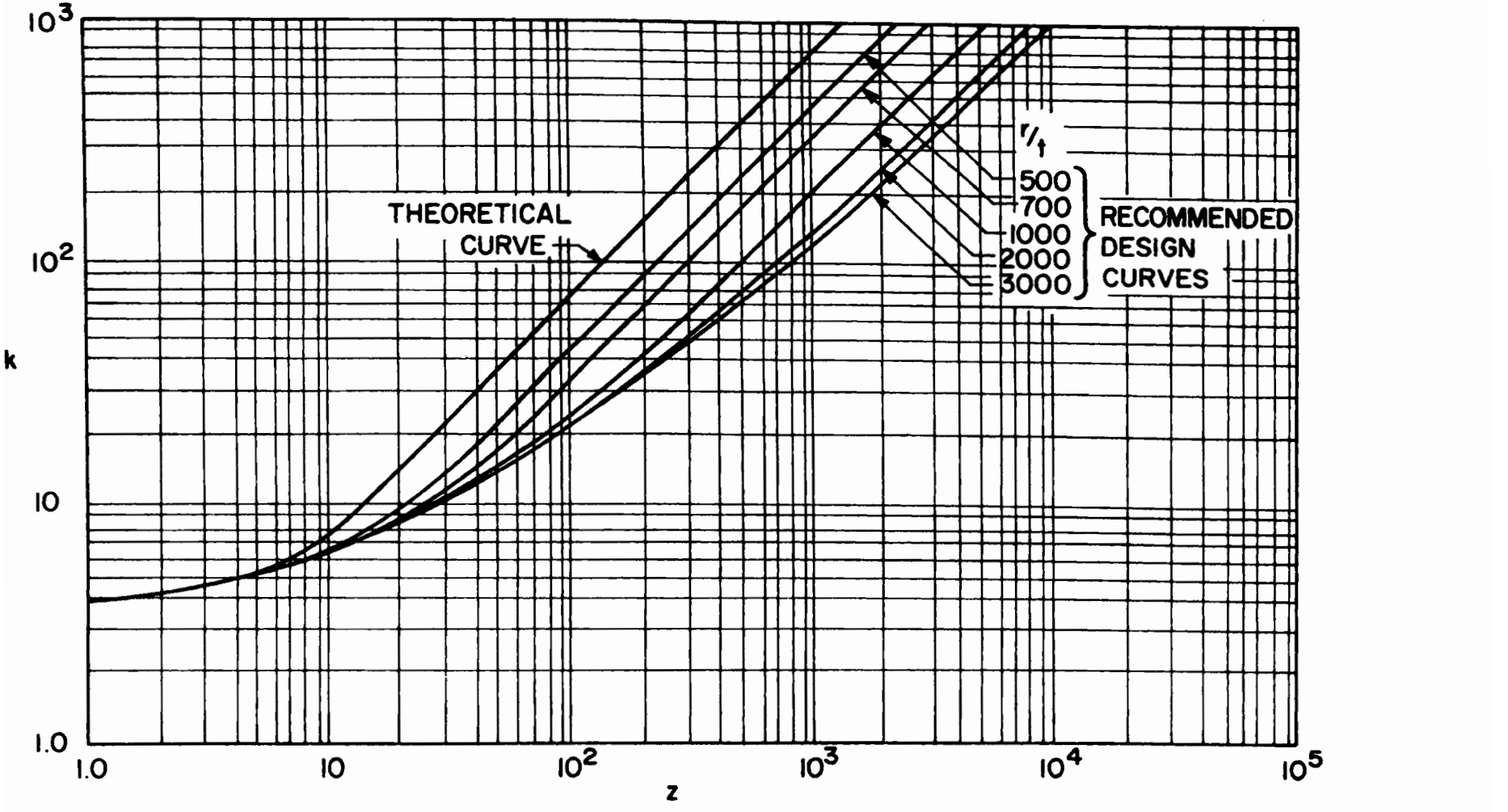

Figure 9. Buckling Coefficients for Transversely Curved Plates

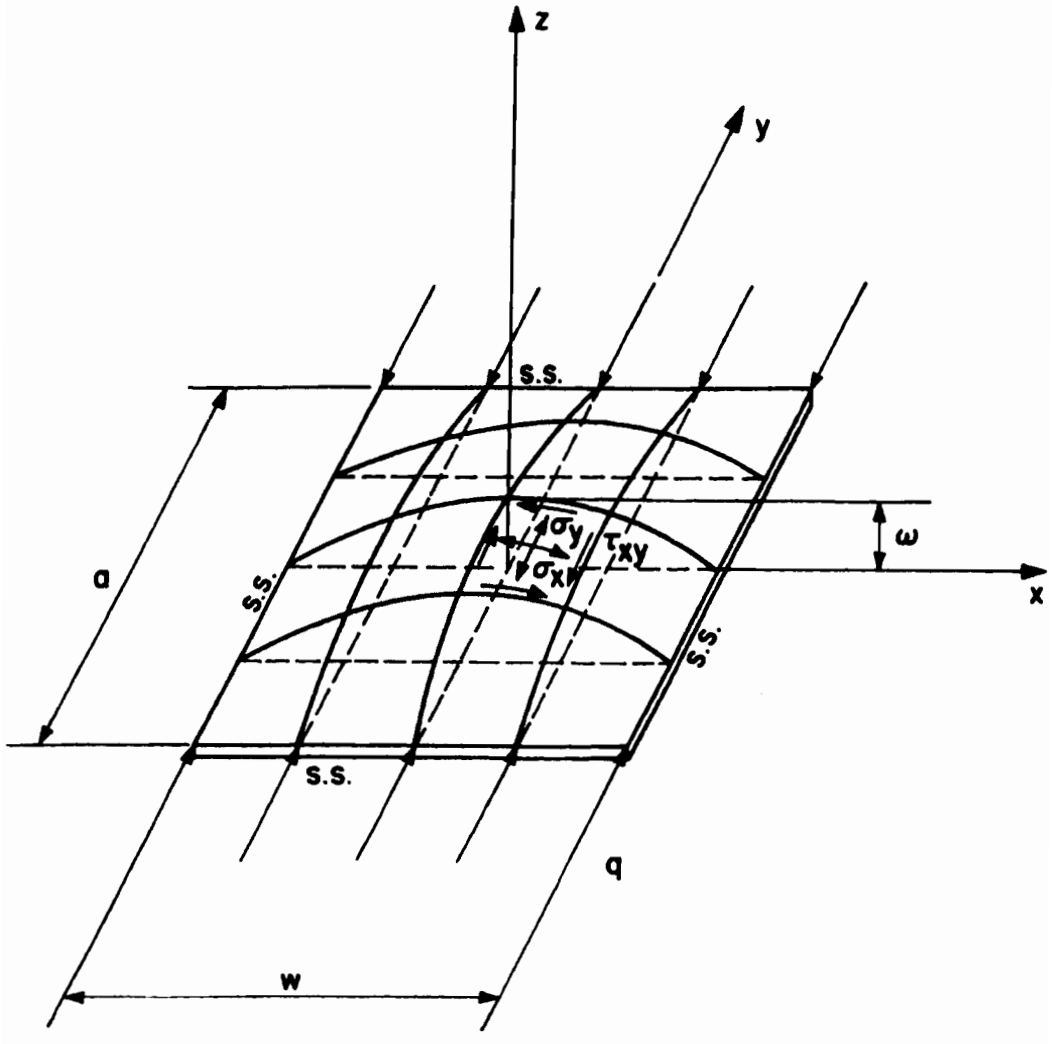

Figure 10. Geometry of a Stiffened Plate

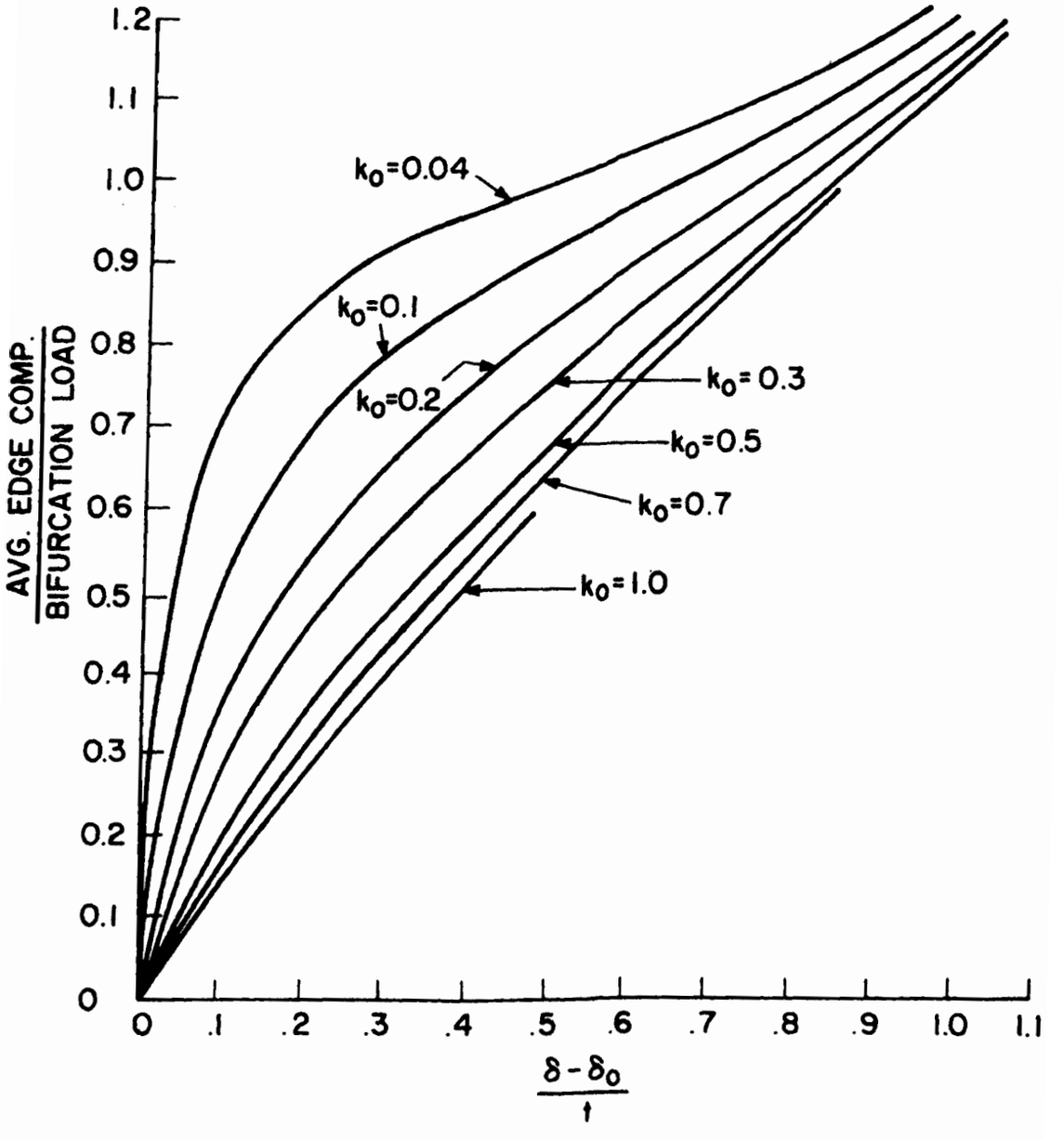

Figure 11. Load-Deflection Curves for Initially Curved Stiffened Elements

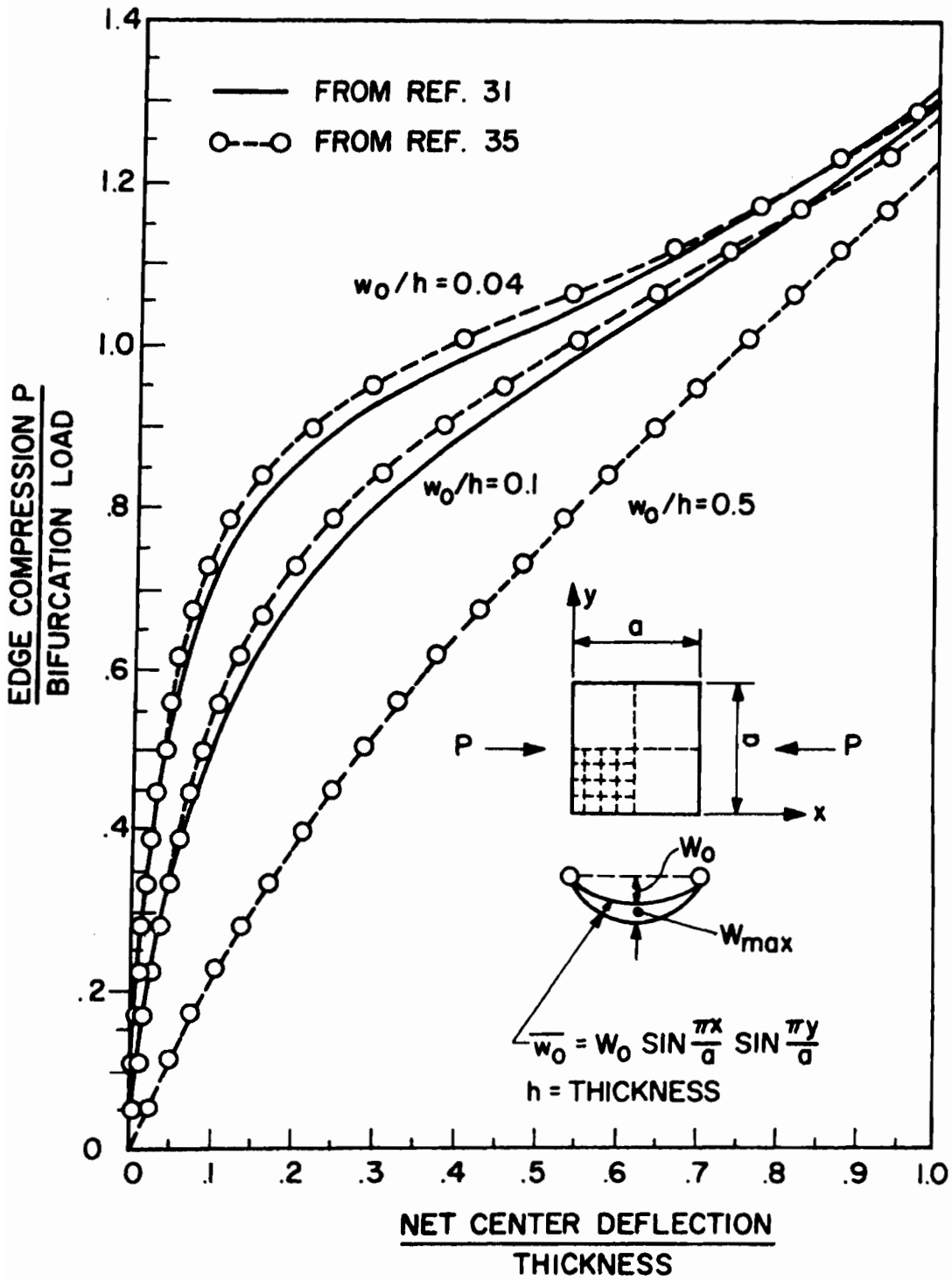

Figure 12. Yang's Load-Deflection Curves

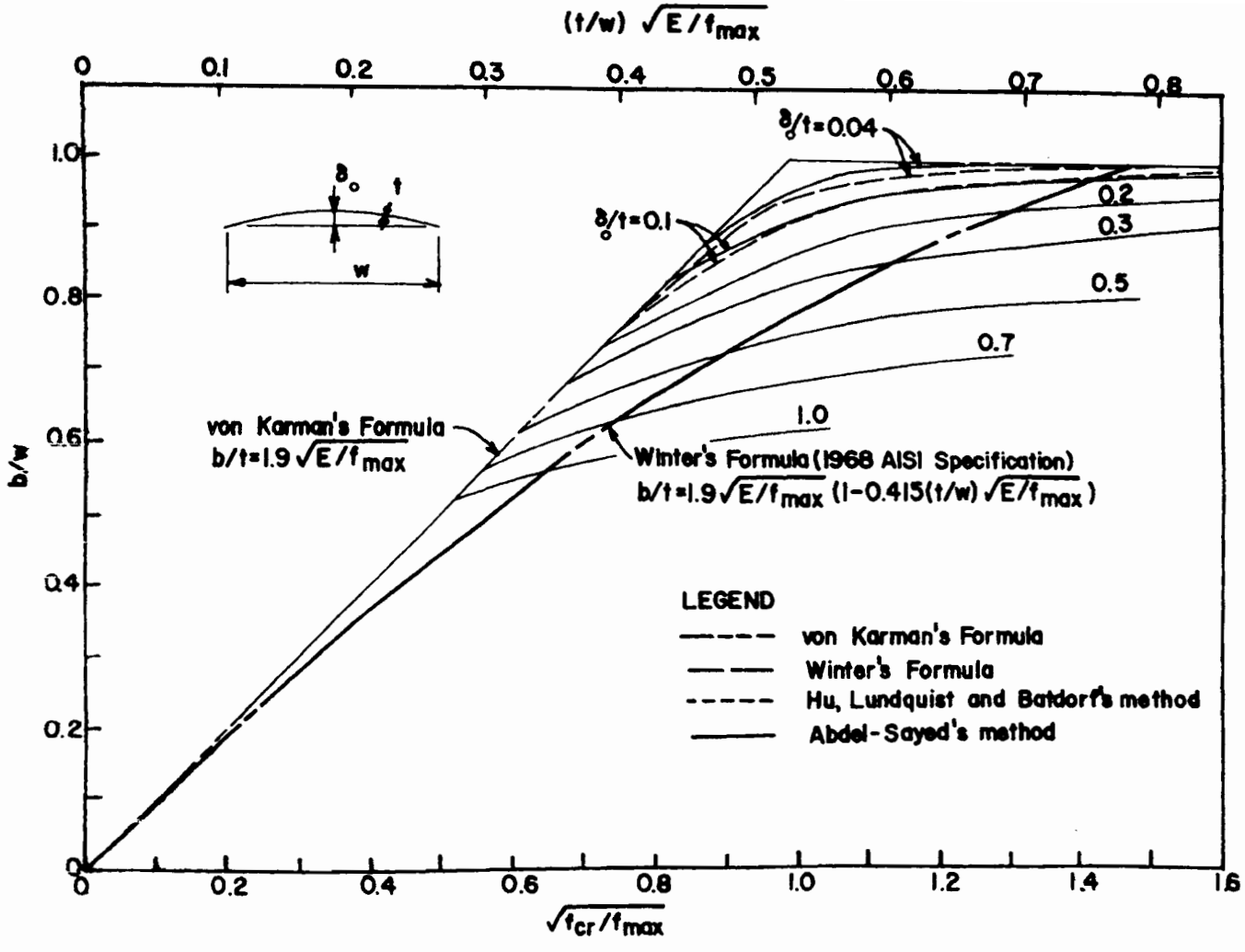

Figure 13. Effect of Initial Deviation from Flatness on Effective Design Width - Equation 3.5

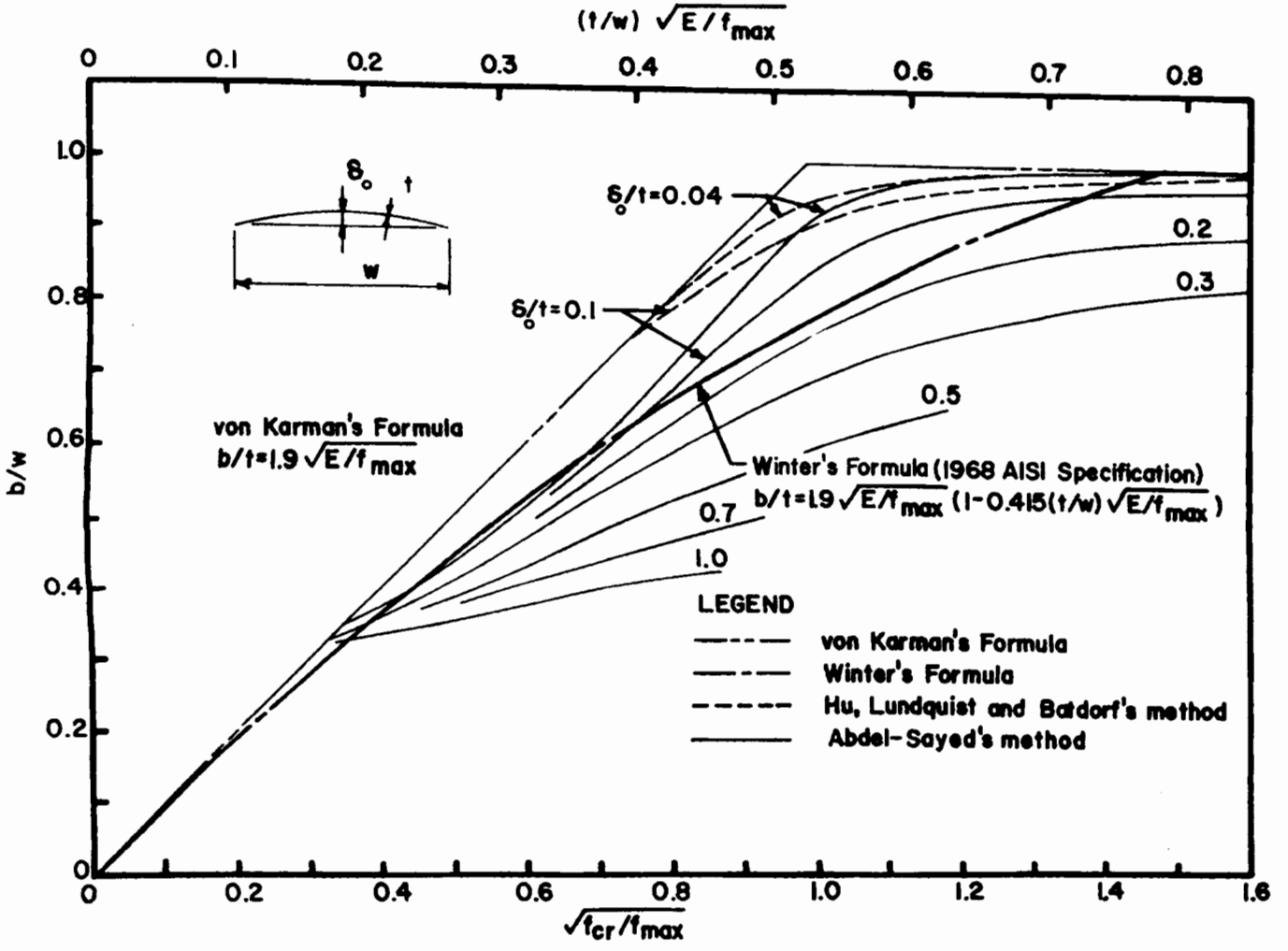

Figure 14. Effect of Initial Deviation from Flatness on Effective Design Width - Equation 3.6

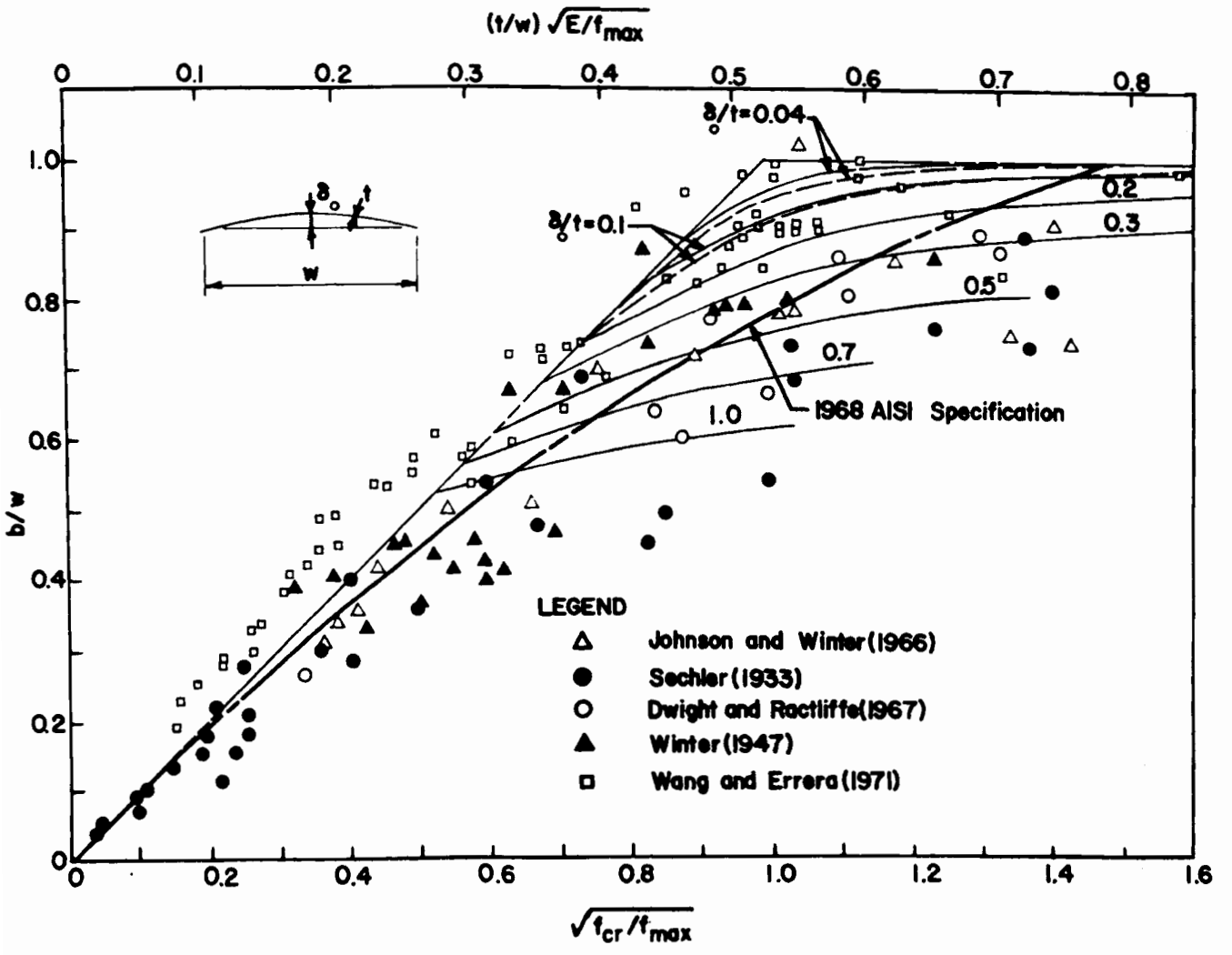

Figure 15. Correlation of Analytical and Experimental Results - Equation 3.5

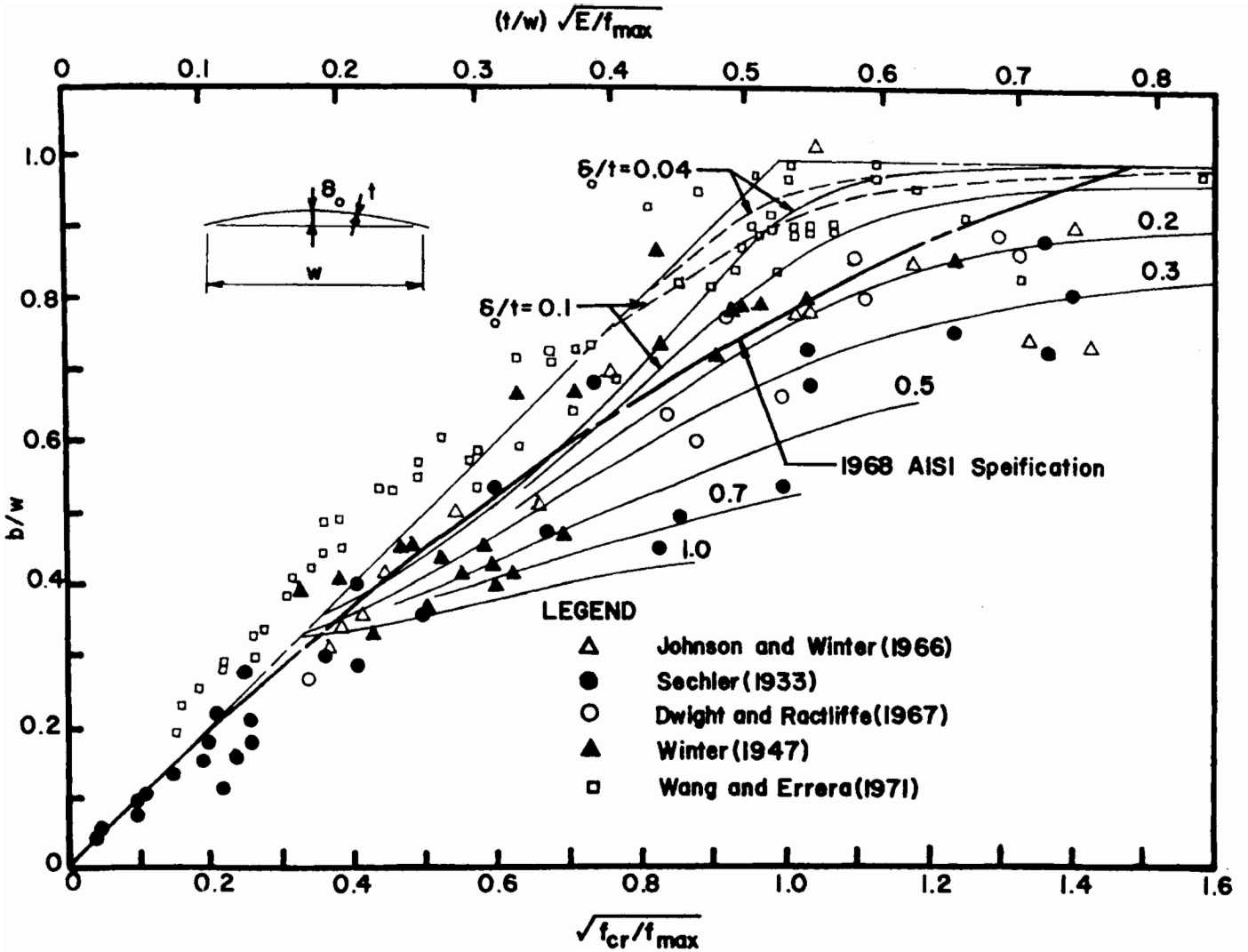

Figure 16. Correlation of Analytical and Experimental Results - Equation 3.6

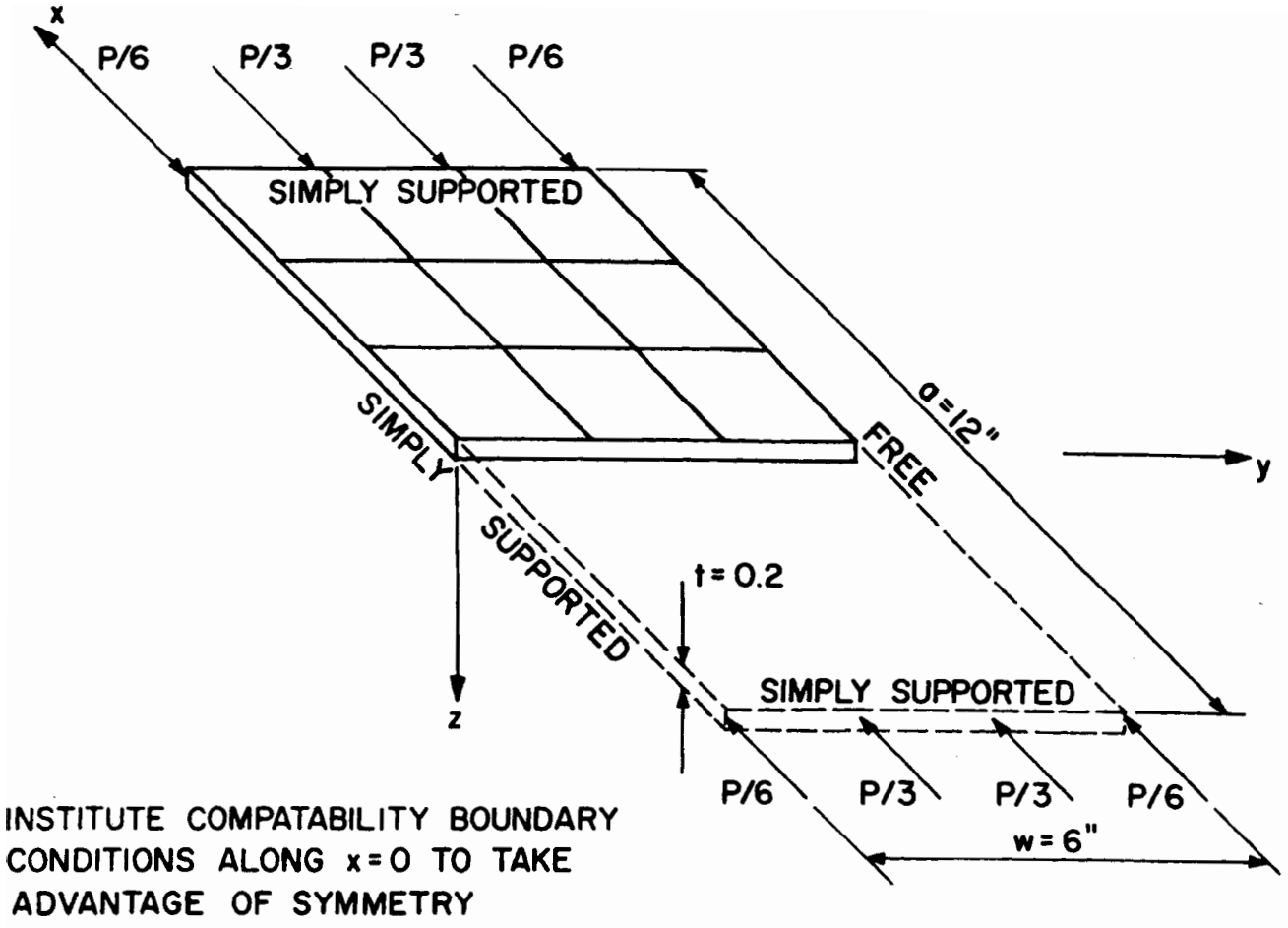

Figure 17. Uniaxially Compressed Unstiffened Element

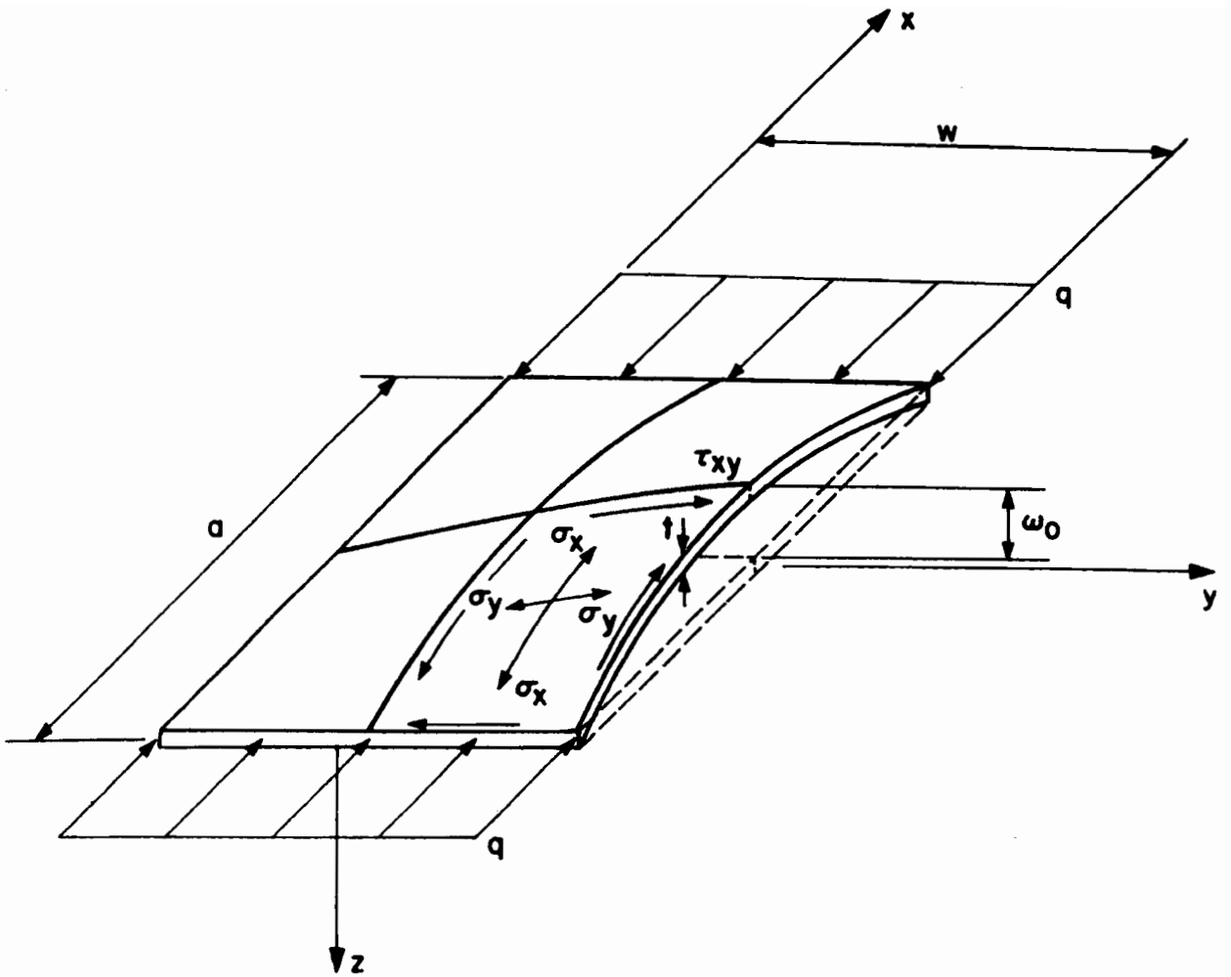

Figure 18. Assumed Deflected Shape for Unstiffened Element

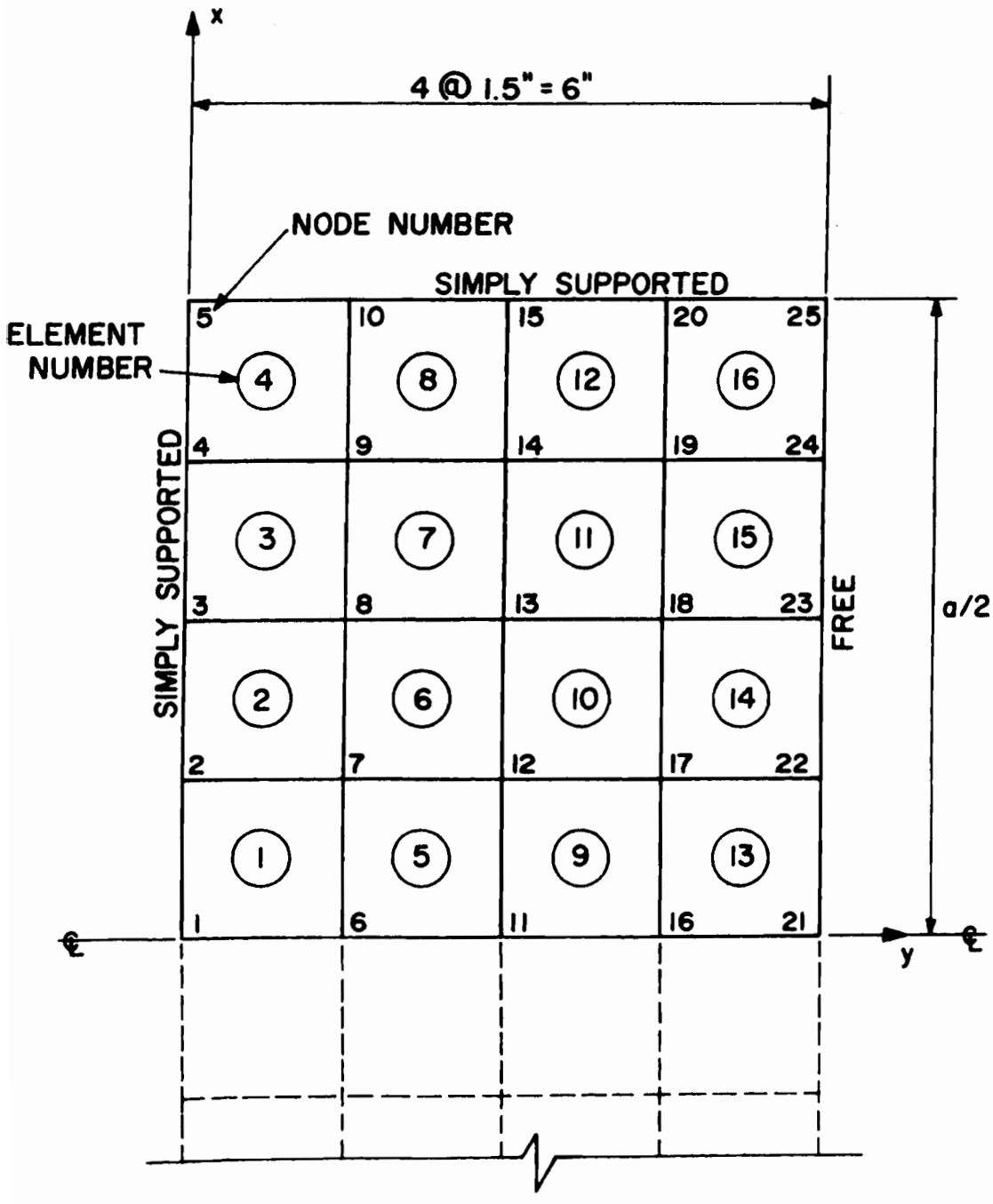

Figure 19. Mesh Generation for Finite Element Analysis

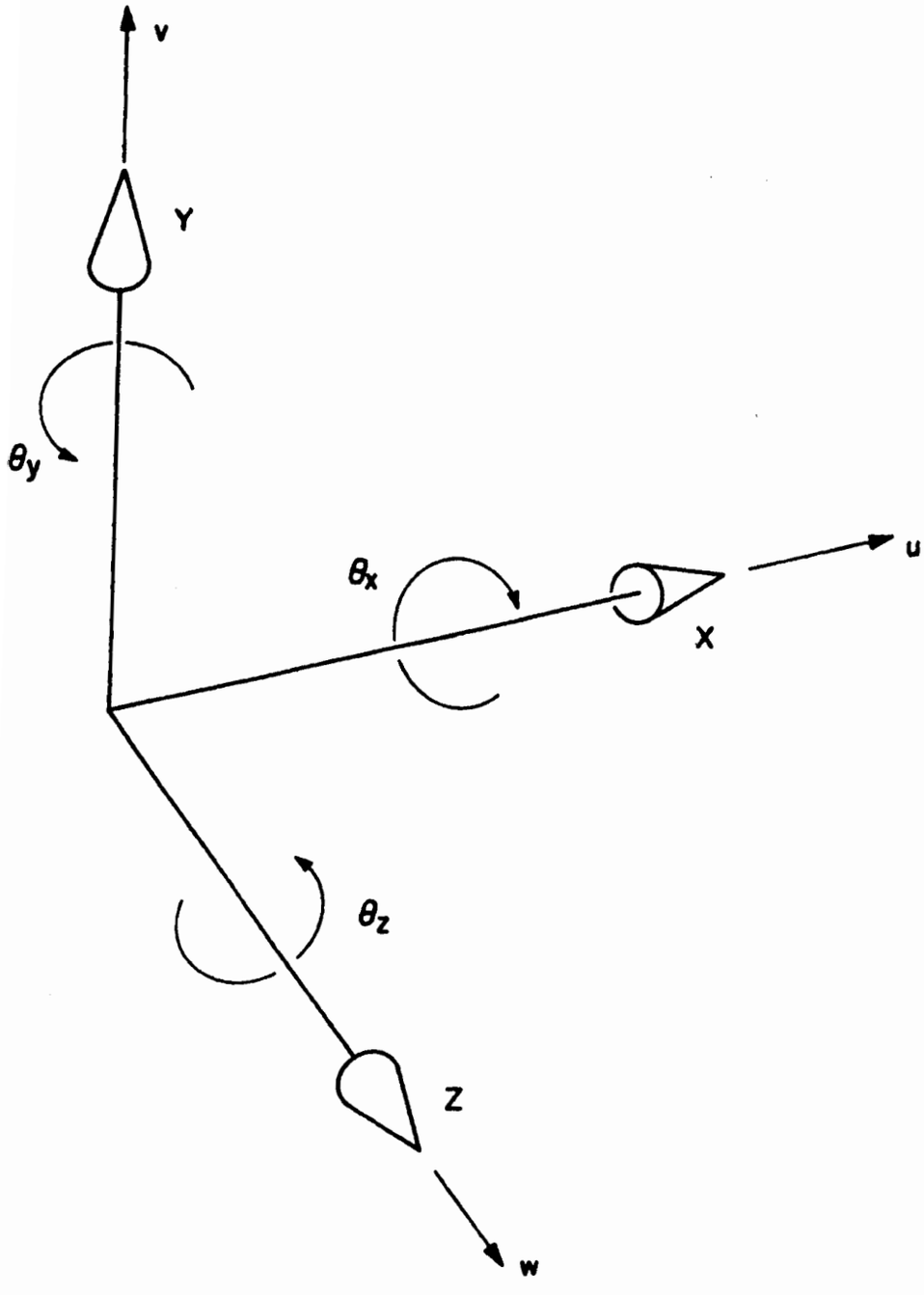

Figure 20. Rotations and Displacements

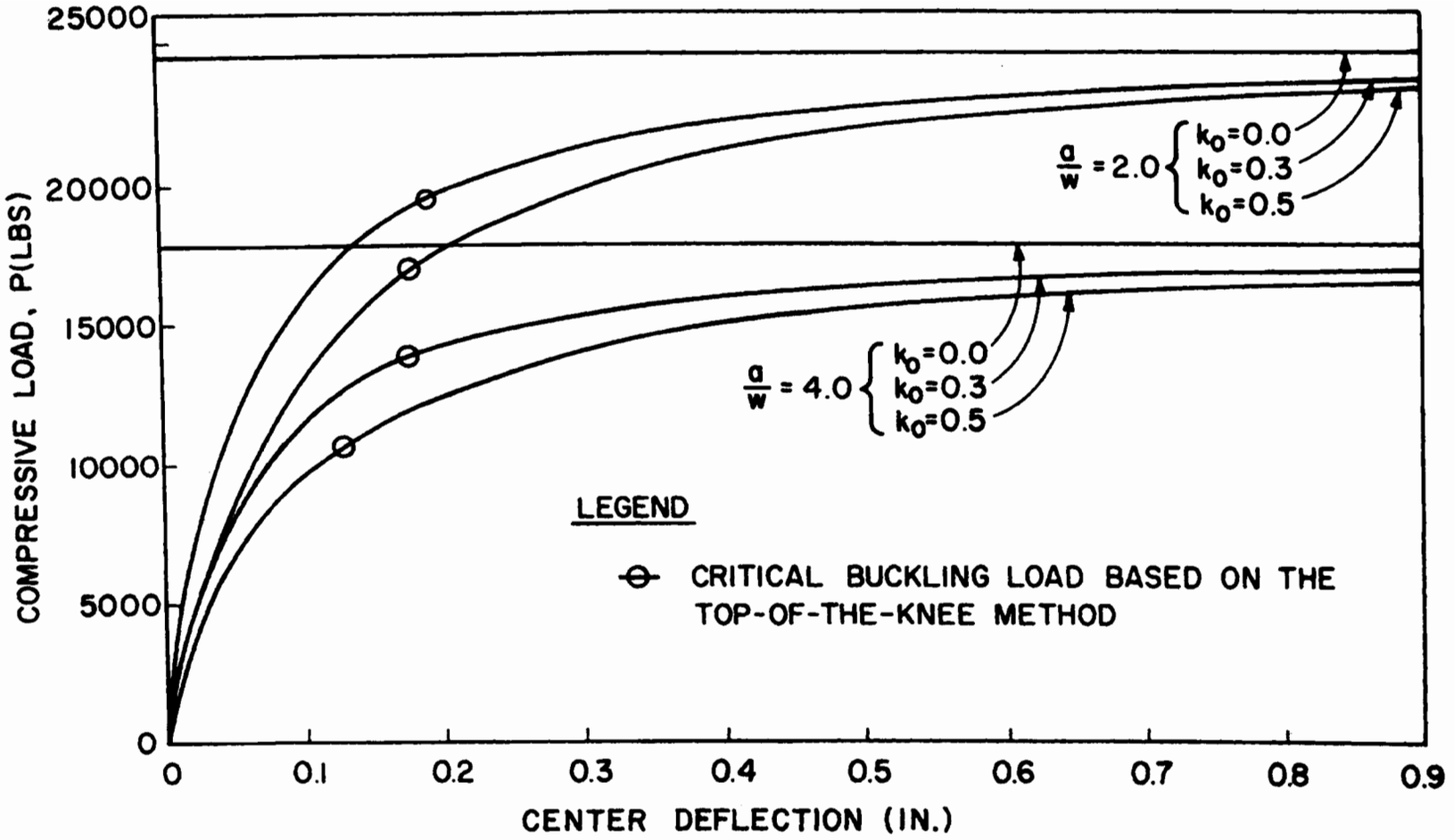

Figure 21. Load-Deflection Curves for Initially Curved Unstiffened Element